Survey of automated multiple sclerosis lesion segmentation techniques on magnetic resonance imaging

Antonios Danelakis[a,*], Theoharis Theoharis[a], Dimitrios A. Verganelakis[b]

[a] *Department of Computer & Information Science, Norwegian University of Science & Technology, Sem Saelands vei 7-9, NO-7491 Trondheim, Norway*
[b] *Nuclear Medicine Department, Oncology Clinic 'ELPIDA', Children's Hospital 'A. Sofia', Goudi Greece.*

Abstract

Multiple Sclerosis (MS) is a chronic disease. It affects the central nervous system and its clinical manifestation can variate. Magnetic Resonance Imaging (MRI) is often used to detect, characterize and quantify MS lesions in the brain, due to the detailed structural information that it can provide. Manual detection and measurement of MS lesions in MRI data is time-consuming, subjective and prone to errors. Therefore, multiple automated methodologies for MRI-based MS lesion segmentation have been proposed. Here, a review of the state-of-the-art of automatic methods available in the literature is presented.

The current survey provides a categorization of the methodologies in existence in terms of their input data handling, their main strategy of segmentation and their type of supervision. The strengths and weaknesses of each category are analyzed and explicitly discussed. The positive and negative aspects of the methods are highlighted, pointing out the future trends and, thus, leading to possible promising directions for future research. In addition, a further clustering of the methods, based on the databases used for their evaluation, is provided. The aforementioned clustering achieves a reliable comparison among methods evaluated on the same databases.

*Corresponding author
Email addresses: antonios.danelakis@ntnu.no (Antonios Danelakis), theotheo@ntnu.no (Theoharis Theoharis), dimitris.verganelakis@gmail.com (Dimitrios A. Verganelakis)

Despite the large number of methods that have emerged in the field, there is as yet no commonly accepted methodology that has been established in clinical practice. Future challenges such as the simultaneous exploitation of more sophisticated MRI protocols and the hybridization of the most promising methods are expected to further improve the performance of the segmentation.

Keywords: Brain MRI, Multiple Sclerosis, Automated Segmentation, Survey

1. Introduction

Multiple sclerosis (MS) is a chronic disease that affects the central nervous system (CNS) with great variability in its clinical manifestation. MS is a progressive neurological disease which changes the morphology and structure of the brain, causing disability in young adults. Depending on the area of the CNS which is affected, symptoms ranging from blurred vision, severe muscle weakness and degradation (Filippi et al., 1995) to coordination and cognitive impairment are observed (Compston and Coles, 2008). MS is relatively common in Europe, the United States and parts of Australia, but rare in Asia. In addition, it is more prevalent in women than men and its incidence increases rapidly after the age of 18, reaches a peak between 25 and 35 and then slowly declines, becoming rare at 50 and older. According to the latest epidemiological studies (Browne et al., 2014; World Health Organization (WHO) and Multiple Sclerosis International Federation, 2008), the frequency of the disease has been increasing worldwide. While the etiology of the disease is not entirely known, environmental factors and genetic effects are considered as the most probable causes (Noseworthy et al., 2000). Although MS does not affect significantly the patients' life duration, there is a substantial impact on the quality of life of the patients and their families.

Conventional MRI is considered as one of the most important modalities of medical imaging and, in general, is an excellent non-invasive imaging technique for studying the brain. MRI is highly sensitive in detecting MS plaques and can provide quantitative assessment of inflammatory activity and lesion load. This

has established MRI as a key clinical tool for diagnosing MS (Fazekas et al., 1999; Simon et al., 2006), assessing the progression (Martola et al., 2010; Rovira and León, 2008; Rovira et al., 2009) and the activity (Tian et al., 2012) of the disease and monitoring the efficacy of medical treatments (Calcagno et al., 2010; Ge, 2006; Van Den Elskamp et al., 2010). The presence and spatial pattern of MS lesions in MRI (dissemination in space) and the appearance of new MS lesions (dissemination in time) are key components of current diagnostic criteria for the disease (Polman et al., 2011). Thus, identifying and segmenting MS lesions is an essential first step in characterizing the disease, and in calculating and interpreting more specialized metrics of damage.

The most common MRI protocols (Hashemi et al., 2012) used in detecting MS lesions are T1-weighted (T1-w), T2-weighted (T2-w), PD-weighted (PD-w) and fluid attenuated inversion recovery T2 (T2-FLAIR)sequences. MS lesions exhibit hyperintensities in T2-w, PD-w and T2-FLAIR MRI sequences, and hypointensities in T1-w MRI sequences, with respect to normal intensities. Figure 1 shows four MRI images (T1-w, PD-w, T2-w, and T2-FLAIR) of a brain with MS lesions.

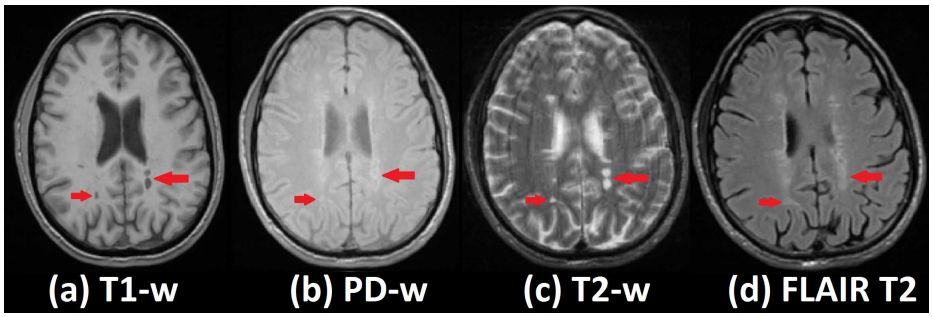

Figure 1: (a) T1-w, (b) PD-w, (c) T2-w, and (d) T2-FLAIR images of a damaged brain. MS lesions are pointed at by red arrows.

Before the advent of computers in radiology, lesions were visually identified and measured by neuroradiologists. However, manual segmentation of MS lesions is a time-consuming and tedious process. In addition, it suffers from subjectiveness and is very prone to human errors. This is what makes an automated

MS lesion segmentation technique an attractive aid for neuroradiologists. The ultimate goal is to obtain an automatic segmentation method that enables the efficient processing of the large amount of information within an MRI. Although many automated MS lesion segmentation methods have been proposed in recent years, no single method is yet widely employed. This is because the aforementioned methods are still encountering technical difficulties. A major difficulty is the overlapping intensity distributions of MS lesions and gray matter of the brain (Sahraian and Radue, 2008). Some regions of the lesion cannot be distinguished from gray matter using either nonparametric or multi-parametric statistical classification techniques. This is due to the heterogeneity of lesions as well as the finite resolution of the images and complicated shapes of the brain tissues that impact a large number of the voxels located on the borders of various tissues (Mortazavi et al., 2012). In addition, although the gap between experts and automated approaches has been decreased during the recent years, automated methods are, in most cases, still outperformed by manual segmentations performed by experts. Thus, there is still room for improvement, in terms of performance. Much work has been done to improve the quality of the automatic segmentation, and newer methods provide more complex approaches to deal with the aforementioned drawbacks. These drawbacks constitute the main reason that research on this field is open and a comprehensive review of the state-of-the-art approaches can prove to be of great importance for researchers who want to improve upon previous work or develop new automated methods.

In the current survey, we explicitly analyze the developed automated MS lesion segmentation approaches through a comprehensive up-to-date state-of-the-art review. To this end, the approaches are categorized, in terms of their main features and properties. Furthermore a qualitative and quantitative comparison of the state-of-the-art approaches is provided, while their strengths and weaknesses are illustrated. The ultimate goal of this survey is to aid in identifying the most promising research directions in the field.

It must be pointed out that there are four very extensive reviews on methodologies published until 2013 (García-Lorenzo et al., 2013; Lladó et al., 2012a;

Lladó et al., 2012b; Mortazavi et al., 2012). In order to keep the length of the current survey within practical limits, the current survey is focused on automated MS lesion segmentation techniques published since 2013; the reader is refereed to the four aforementioned surveys for techniques published up to 2013. Thus, not only a novel categorization of the related techniques is provided, but also the techniques, illustrated in the current review, are not included in the existing surveys. The bibliography is very rich and a relatively large number of new methods have been published since 2013. Table 1 summarizes the number of state-of-the-art methodologies reviewed by the previous as well as the current survey. As the previous four surveys were published at a similar time, there is a great overlap between the reviewed methods between them.

SURVEY	PUBLISHED	# OF METHODS REVIEWED
(Mortazavi et al., 2012)	2012	44
(Lladó et al., 2012b)	2012	34
(Lladó et al., 2012a)	2012	34
(García-Lorenzo et al., 2013)	2013	55
Current Survey	2018	45

Table 1: Number of methodologies reviewed in the previous and the current survey.

Providing a reliable comparison of the state-of-the-art methodologies includes some objective difficulties. These stem from the fact that the existing methodologies employ different evaluation measures and different MS lesion databases. Ideally, all methods would be applied on a common database and its accompanying ground truth. Then, the techniques would be directly and reliably comparable using the same evaluation measures. However, due to the public unavailability of the source code of most methodologies and the lack of large-scale publicly available databases of real images along with their ground truth, this ideal situation cannot be achieved at present. Consequently, throughout the current survey, the state-of-the-art methodologies will be compared according to their reported results and evaluation measures, as per the literature. Fortunately, the recent establishment of MS Lesion Segmentation Challenges

(Carass et al., 2017; Commowick et al., 2016; Styner et al., 2008) has provided a common framework for MS lesion segmentation algorithms, allowing reliable and direct comparisons to be made between different approaches.

The rest of this survey is organized as follows: In Section 2, the publicly available MS lesion databases as well as the most common evaluation measures for MS lesion segmentation techniques are illustrated. Section 3 reviews the state-of-the-art automated MS lesion segmentation methodologies. Section 4 provides a qualitative and quantitative comparison of the aforementioned state-of-the-art methodologies. A discussion, where directions for future research in the field are drawn, is given in Section 5. Future challenges and suggestions are highlighted in Section 6.

2. Materials

2.1. MS lesion databases

Due to the lack of large-scale publicly available databases and corresponding ground truth data that can be used to benchmark MS lesion segmentation methodologies, the comparison of the state-of-the-art approaches is a bit tricky. Ideally, all the approaches should be tested on the same benchmark database(s) providing direct and reliable comparisons. Many state-of-the-art methodologies use their own proprietary database raising questions of reproducibility.

In recent years, there has been some progress towards the creation of benchmark MRI databases for MS lesion segmentation techniques. $MICCAI$ and $ISBI$ MS Lesion Segmentation Challenges (Carass et al., 2017; Commowick et al., 2016; Styner et al., 2008) provided common databases that were used by some of the state-of-the-art approaches for evaluation. Techniques that were tested on these databases can be compared more reliably. At this point it has to be pointed out that reports that stem out of such challenges do not contain a birds eye view of the field since they are restricted only to the papers that participate to these challenges.

The $MICCAI$ 2008 (Styner et al., 2008) database consists of MRI images acquired by a $3T$ Siemens Allegra system. The data were fully anonymized for dissemination purposes. Eventually, the database was segmented by three expert raters. The evaluation is performed against all the experts' results. The participants were provided with 20 training cases with manual segmentations from one of the experts and 25 testing cases without expert segmentations. The subjects of the database were randomly assigned to training and testing. The database contained the same number of high resolution T1-w weighted, T2-w and T2-FLAIR. All the images were given the same axial orientation and were appropriately processed, in terms of registration and interpolation, to be more easily manageable by the participants.

In $MICCAI$ 2016 (Commowick et al., 2016), the data were acquired by many different MRI scanners using different magnetic field strengths. A $3T$ Siemens Aera $1.5T$, a Siemens Verio $3T$, a Philips Ingenia $3T$ and a General Electric Discovery $3T$ were used. Once again, the images were pre-processed for the convenience of the participants. The data were also anonymized. The participants were provided with 15 training cases and 38 testing cases, randomly selected. The training cases were accompanied by their ground truth manual segmentations. The database contained T1-w weighted, T1-w gadolinium enhanced (T1-w Gd), T2-w, T2-FLAIR and PD-w images.

Although $ISBI$ 2015 (Carass et al., 2017) data set deals with longitudinal MS lesions, it has been used for validating automatic MS lesion segmentation techniques. In this case, the longitudinal of the data set can be disregarded as the annotation of the data has been performed manually and independently. In $ISBI$ 2015, the data were acquired using a $3T$ Philips Medical Systems MRI scanner. The data were anonymized and the participants were provided with 5 training cases and 14 testing cases, randomly selected. The training cases were accompanied by their ground truth segmentations. The database contained high resolution T1-w weighted, T2-w, T2-FLAIR and PD-w images. Once again, the images were pre-processed for the convenience of the participants.

In the case of the *Whole Brain Atlas* database (Summers, 2003), there

is no available information on the MRI scanner used in order to acquire the anonymous MRI data. This database consists of 100 subjects along with their labeled ground truth. The MRI image sequences acquired are T1-w weighted, T2-w and PD-w.

The aforementioned databases contain real clinical data from real patients. A different approach is the creation of synthetic databases. In this case, the images are synthesized based on a small number of real data. This is very useful for the creation of big databases, as the available real clinical data are restricted. $BrainWeb$ (Cocosco et al., 1997; Collins et al., 1998; Kwan et al., 1996, 1999), is the first effort in this direction. It produced three different MRI image sequences (T1-w, T2-w and PD-w) for normal or MS diseased subjects. The technical characteristics of the produced sequences are determined by the user. More precisely, the user can determine the desired MRI image sequence, the slice thickness, the noise and the intensity non-uniformity (RF). All the possible combinations can produce data for a maximum of 270 virtual patients.

In Table 2, the publicly available MRI databases for MS lesion segmentation evaluation are illustrated. At this point, it must be highlighted, that the three public databases have an important drawback; they are small scale. Thus, the question of reproducibility of the results of the techniques evaluated on these databases, still remains.

DATABASE	PUBLISHED	NR OF SUBJECTS	*MRI* SEQUENCES	*MRI* SCANNER
BrainWeb (Cocosco et al., 1997)	1997	270	T1-w, T2-w, *PD*-w	Synthetic
Whole Brain Atlas (Summers, 2003)	2003	100	T1-w, T2-w, *PD*-w	N/A
MICCAI 2008 (Styner et al., 2008)	2008	45	T1-w, T2-w, T2-FLAIR	3*T* SIEMENS
ISBI 2015 (Carass et al., 2017)	2015	19	T1-w, T2-w, T2-FLAIR, *PD*-w,	3*T* PHILIPS
MICCAI 2016 (Commowick et al., 2016)	2016	53	T1-w, T2-w, T2-FLAIR, *PD*-w, T1-w *Gd*	1.5*T* SIEMENS
				3*T* SIEMENS
				3*T* PHILIPS
				3*T* GE

Table 2: Publicly available databases for MRI-based MS lesion segmentation evaluation.

2.2. Evaluation measures

A variety of measures are used in the literature to evaluate the automated methods proposed for the segmentation of MS lesions. All of these measures

are based on comparing the result of the automated segmentation against the ground truth. In order to comprehend the evaluation measures, four basic retrieval terms and their clinical meaning should be understood (Goldberg-Zimring et al., 1998):

- *True Positive* (TP): Refers to correctly segmented MS lesions areas.
- *True Negative* (TN): Refers to correctly rejected MS lesions areas.
- *False Positive* (FP): Refers to incorrectly segmented MS lesions areas.
- *False Negative* (FN): Refers to incorrectly rejected MS lesions areas.

With the above terminology in mind, the evaluation measures used in the segmentation techniques are concisely presented in Table 3. Each measure is followed by its mathematical calculation and a description when needed. It should be noted that all these measures are closely related. Sometimes, different researchers used the same evaluation measure under different names. This fact is taken into account in the last column of Table 3.

The above measures can be classified into five main groups:

- Deterministic measures: Each voxel is assigned to only one tissue type.
- Probabilistic measures: Each voxel has a membership value for belonging to the different tissue types.
- Area measures: Compare areas of automatically detected segments to the ground truth areas.
- Volume measures: Compare volumes of automatically detected segments to the ground truth volumes.
- Distance measures: Evaluate how far the boundaries of an obtained lesion segmentation are from those of the ground truth.

Table 4 summarizes the classification of the evaluation measures.

MEASURE	CALCULATION	DESCRIPTION	ALTERNATIVE NAMES
Sensitivity (SEN) (Goldberg-Zimring et al., 1998)	$SEN = \frac{TP}{FN+TP}$		*Overlap Fraction*, *True Positive Rate*, *Recall*
Specificity (SPE) (Goldberg-Zimring et al., 1998)	$SPE = \frac{TN}{TN+FP}$		*True Negative Rate*
Accuracy (ACC) (Wu et al., 2006)	$ACC = \frac{TP+TN}{TP+TN+FP+FN}$		
Dice Similarity Coefficient (DSC) (Dice, 1945)	$DSC = \frac{2TP}{2TP+FP+FN}$		F_1 *Score*
Positive Predictive Value (PPV) (Altman and Bland, 1994)	$PPV = \frac{TP}{TP+FP}$		*Precision*, *Reliability*
Fallout ($FALL$) (Udupa et al., 2006)	$FALL = 1 - SEN = \frac{FP}{FP+TN}$		*False Positive Rate*, *False Alarm Ratio*
Extra Fraction (EF) (Stokking et al., 2000)	$EF = \frac{FP}{TP+FN}$		
Detection Error Rate (DER) (Wack et al., 2012)	$DER = \frac{DE}{MTA}$	DE: Detection Error MTA: Mean Total Area	
Outline Error Rate (OER) (Wack et al., 2012)	$OER = \frac{OE}{MTA}$	OE: Outline Error MTA: Mean Total Area	
Correct Detection Ratio (CDR) (Roy et al., 2015)	$CDR = \frac{TP}{MS}$	MS: manually segmented area	
False Detection Ratio (FDR) (Roy et al., 2015)	$FDR = \frac{AS-TP}{MS}$	AS: automatically segmented area	
Relative Area Error (RAE) (Roy et al., 2015)	$RAE = \frac{AS-MS}{MS}$		
Jacard Index (JI) (Roy et al., 2015)	$JI = \frac{TP}{TP+FN+FP}$		
Volume Difference (VD) (Cárdenes et al., 2009)	$VD = \frac{FN-FP}{2TP+FP+FN}$		
Intra-Class Correlation (ICC) (Koch, 1982)	$ICC = \frac{\sigma_S^2}{\sigma_S^2+\sigma_\epsilon^2}$	σ_S^2: differential variance between the segmentations σ_ϵ^2: differential variance between the points in the segmentations	
Hausdorf Distance (HD) (Gerig et al., 2001)	$HD(A,B) = max(h(A,B), h(B,A))$	$h(A,B) = max_{a\in A} min_{b\in B} \|\|a-b\|\|$ $\|\|a-b\|\|$: the Euclidean distance A, B: two finite sets	
Average Distance (AD) (Khotanlou et al., 2009)	$AD(A,B) = max(d(A,B), d(B,A))$	$d(A,B) = \frac{1}{N}\sum_{a\in A} min_{b\in B} \|\|a-b\|\|$ $\|\|a-b\|\|$: the Euclidean distance A, B: two finite sets N: number of elements of the finite sets	
Pearson's r Coefficient (PrC) (Bland, 2015)	$PrC = \frac{\sum_{i=1}^{N}(x_i-\overline{x})(y_i-\overline{y})}{\sqrt{\sum_{i=1}^{N}(x_i-\overline{x})^2}\sqrt{\sum_{i=1}^{N}(y_i-\overline{y})^2}}$	N: number of time points x_i, y_i: volumes of the ground truth and the automatic segmentation $\overline{x}$, $\overline{y}$: respective means of the absolute volumes	

Table 3: Evaluation measures for the reviewed automated MS lesion segmentation techniques.

DETERMINISTIC	PROBABILISTIC	AREA	VOLUME	DISTANCE
SEN	ICC	DER	VD	HD
SPE	PrC	OER		AD
ACC		RAE		
DSC		CDR		
PPV		FDR		
$FALL$				
EF				
JI				

Table 4: Classification of evaluation measures for automated MS lesion segmentation.

It must be pointed out that there are many more evaluation metrics for segmentation but in the current survey, only the set of measures which are used in the reviewed techniques presented in Section 3, are illustrated. For more evaluation metrics and corresponding categories on medical image segmentation, the reader is refereed to (Taha and Hanbury, 2015). Note that most measures are deterministic followed by area measures, distance measures, probabilistic measures and volume measures. It appears that the DSC measure is the most prolific one for evaluating MS lesion segmentation methods, as it is the only evaluation measure in common among all the reviewed methodologies.

3. Methods

A categorization of the state-of-the-art methodologies is first suggested and a review of the methodologies follows, based on the given categorization. The review emphasizes on the steps that differentiate the methodologies.

3.1. Categorization of Methodologies

Although it is hard to explicitly categorize the state-of-the-art MRI-based MS lesion segmentation techniques because of large overlaps between them, we have formulated categories based on the following characteristics that all methods have:

- Input data handling.
- Main strategy.
- Existence of supervision.

With respect to the input data handling, the following classification is suggested:

- $3D$ volume-based methodologies: The input data represent the $3D$ volume of the patient's brain. Such methodologies process data at voxel level. Some of the methods of this category are able to directly perform $3D$ segmentation.
- $2D$ image -based methodologies: The data represent the sequence of $2D$ MRI images of the patient's brain. The methodologies belonging to this category, process data at pixel level. They implement $2D$ segmentation on each image, and then, they are able combine the individual image segmentations in order to provide the final $3D$ segmentation.

For the main strategy of the methodologies the following six categories are suggested:

- Data-driven methodologies: These methods implement data-based approaches such as thresholding, spatial analysis, intensity analysis, morphology analysis topology analysis or region growing.
- Feature-based methodologies: These methods extract features, that can be used to model the input data. These features are meant to contain all the meaningful information of the initial data and, thus, represent an explicit representation that can be used for further processing.
- Atlas-based methodologies: An atlas is a brain map providing either statistical or topological information. A statistical atlas provides the prior probability of each voxel belonging to a particular tissue class. On the

other hand, a topological atlas encodes a specific topology for each structure and group of structures. Methodologies that use atlas information require the application of a registration process in order to fit the atlas to the input data.

- Statistical methodologies: The methods of this category exploit estimation of probability density functions which lead to probabilistic segmentation.
- Tissue-based methodologies: These methods segment the normal tissues of the brain first and then the MS lesions appear as outliers on each normal tissue.
- Lesion-based methodologies: This group of methods either directly segment the lesions or they segment the lesions simultaneously with normal tissues.

Finally, with respect to supervision, two categories exist:

- Supervised methodologies: These methods implement a training process in order to learn the definition of lesions from exemplary data, previously segmented by another method. The exemplary data is usually manually segmented. The training is based on the features extracted by the methodologies. The main feature extraction strategies of the supervised methods recruit atlas-based, data-driven or statistical methodologies.
- Unsupervised methodologies: These methods do not require labeled training data to perform the segmentation. Most of these methods employ clustering techniques to separate the voxels (or pixels) into different classes (or clusters) based on different extracted features. Typically, these clusters are then assigned to White Matter (WM), Gray Matter (GM), Cerebrospinal Fluid (CSF), or MS lesion according to some a priori information.

Figure 2, illustrates the proposed categorization of the state-of-the-art MS lesion segmentation techniques. Figures 3 and 4 illustrate the collective generalized pipeline of supervised and unsupervised MS lesion segmentation methodologies respectively.

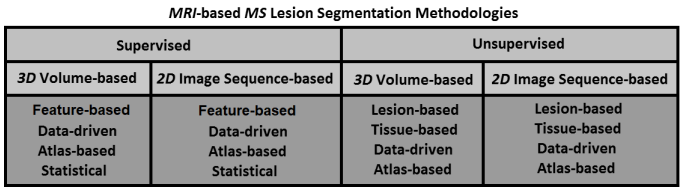

Figure 2: Proposed categorization of state-of-the-art MS lesion segmentation methodologies.

3.2. Review of Methodologies

The review is focused on the steps that differentiate the methodologies and is structured according to the proposed categorization. Note that some methods could be categorized into multiple categories; the category that is closest to the core algorithm that the method implements is used.

3.2.1. Supervised Methodologies

3.2.1.1. 3D Volume-based Methodologies.

3.2.1.1.1. Feature-based Methodologies

In (Jog et al., 2015), all images undergo pre-processing including $N4$ bias correction (Tustison et al., 2010), rigid registration (Collins et al., 1995) and skull stripping (Carass et al., 2011). Then, segmentation takes place using trained multi-output decision trees. As training features, besides the local intensity information which is unable distinguish between lesion and normal tissue alone, features that provide global context for a voxel are also recruited. Finally, the membership image acquired from the multi-output decision ensemble is smoothed using a Gaussian filter in order to reduce false positives.

Intensity, spatial and symmetry features obtained by multimodal MRI data, are used to train a Random Forest (RF) classifier in method (Geremia et al., 2013). RF aims at automatic semantic labeling of the input MRI data. During training, it learns the optimal image sampling associated with the classification task. During testing, the algorithm quickly handles the background and focuses

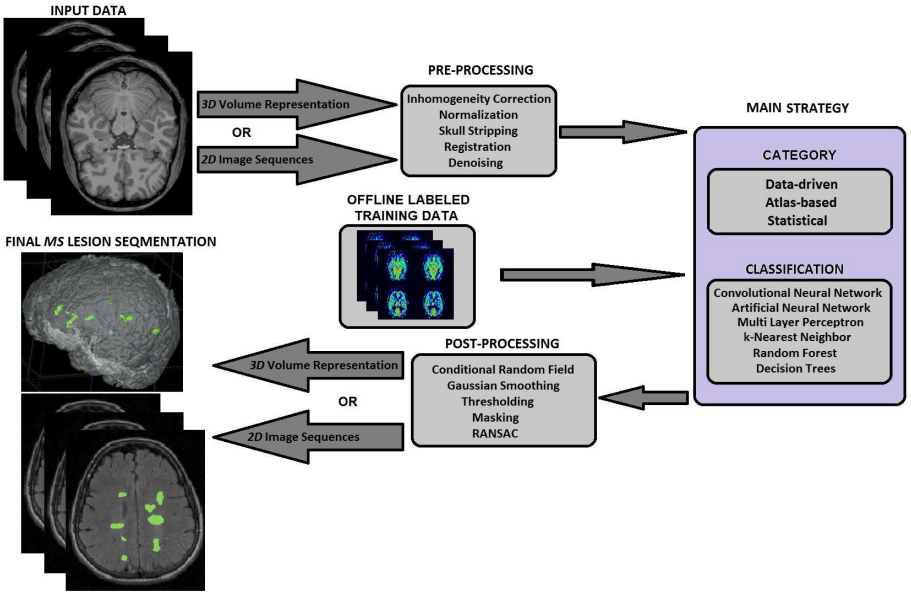

Figure 3: Generalized pipeline of supervised MRI-based state-of-the-art MS lesion segmentation methodologies. Parts of the image were published in (Lladó et al., 2012b) (usage permission granted by authors and publisher).

on challenging image regions to refine the classification.

The method in (Strumia et al., 2016) implements the algorithm presented in (Li et al., 2009) in order to perform inhomogeneities' correction and healthy tissue segmentation at the same time. Then the topological features of MS lesions are used for training. Thus, the aforementioned features are modeled on a geometric brain model which is implemented for recognizing and segmenting the MS lesions.

In (Maier and Handels, 2015), intensity standardization is implemented as a pre-processing step. A RF classifier is trained on spatial features of the voxels. A total of 200 trees are trained without any growth-restriction. To obtain a binary segmentation mask, the output of the RF classifier is thresholded. Finally, single unconnected lesion voxels are removed, holes in binary lesion objects are closed and a single-iteration closing operation with a $3D$ square-connected component is applied.

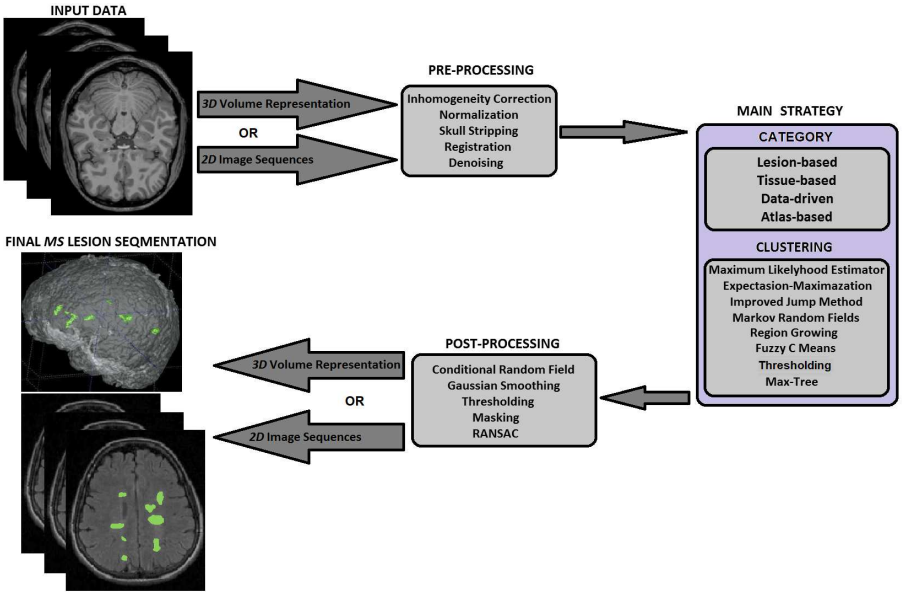

Figure 4: Generalized pipeline of unsupervised MRI-based state-of-the-art MS lesion segmentation methodologies. Parts of the image were published in (Lladó et al., 2012b) (usage permission granted by authors and publisher).

In (Steenwijk et al., 2013) intensity and spatial features are first extracted; the latter are normalized based on robust range normalization (De Boer et al., 2009) and histogram matching (Lao et al., 2008; Younis et al., 2008). Then, Multi-Atlas segmentation (Aljabar et al., 2009) obtains prior probabilistic maps indicating the positioning of the CSF, WM and GM structures of the brain. These maps are called Tissue Type Priors (TTP). The extracted features along with the TTPs create the training vector for a k-Nearest Neighbor ($k-NN$) classifier. The classifier is used to decide whether a voxel is a lesion or not. Finally, a post-processing step is implemented which reduces false positives based on the lesion volumes.

The method proposed in (Mahbod et al., 2016) employs a rich pre-processing step on the initial MRI data which includes histogram matching (Yoo et al., 2002), intensity inhomogeneity correction, extremely low intensity values removal and normalization. Then, intensity-based and spatial-based features are

extracted and imported to a supervised Artificial Neural Network (ANN) classifier. Finally, the ANN performs a per voxel segmentation.

In (Muschelli et al., 2016), the initial MRI images were corrected, using the $N4$ inhomogeneity correction (Tustison et al., 2010). Then, image predictors are derived, based on the pre-processed input MRI image sequences. These predictors exploit features such as the normalized intensity of the voxels, their neighborhood and their contralateral differences. Finally, an RF classifier (Breiman, 2001) is trained in order to provide the probability that a voxel belongs to a lesion.

After the harmonization of every input MRI image sequence intensity, the authors of (Vera-Olmos et al., 2016) extract a number of intensity-based and location-based features. These features are used to train an RF classifier (Buitinck et al., 2013). This classifier derives an initial lesion mask and a lesion probability mask. These masks are exploited by a Markov Random Field (MRF) model in order to grow lesion areas through mask-indicated probable neighborhoods.

3.2.1.1.2. Data-driven Methodologies

(Prados et al., 2015) exploits the multimodal characteristic intensity difference between MS lesions and normal tissues. The Optimized PAtchMatch Label ($OPAL$) fusion approach (Ta et al., 2014) is used to locate pathological regions using a template library comprising a series of multimodal $3D$ images with manually segmented MS lesions. By matching patches between the target multimodal $3D$ image and the multimodal $3D$ images in the template library, $OPAL$ can provide a rough estimate of the location of the lesions in the target image.

The method in (Iheme and Unay, 2015) is based on intensity thresholding and $3D$ voxel connectivity analysis. Voxels that exceed the threshold defined by the authors, are segmented as MS lesions. The $3D$ connectivity analysis involves examining every detected voxel for the degree of connectivity with each

of its neighboring voxels. The training data was used to determine a minimum volume for lesions; connected components that are below this volume threshold are deemed insignificant and assumed to be false positives. To further reduce the incidence of false positives, the interhemispheric fissure is estimated using a $RANSAC$-based approach (Ekin, 2006). Lesions that fall within a prescribed distance of the interhemispheric fissure are also removed as false positives.

Technique (Guizard et al., 2015) implements data denoising (Coupé et al., 2008), $N3$ inhomogeneities' correction (Sled et al., 1998), multimodal MRI data registration and skull-stripping (Eskildsen et al., 2012). The NLM algorithm (Coupé et al., 2008) is enriched by using a rotation-invariant distance metric, instead of the $L2$-norm metric. The aforementioned procedure accurately captures the MS lesion spatial distribution which is used for system training. Thus, lesions of various orientation, shape or size can be detected.

3.2.1.1.3. Atlas-based Methodologies

The methodology presented in (Jesson and Arbel, 2015) performs intensity normalization and denoising, based on a non-local mean method (Coupé et al., 2008), as pre-processing steps. Then, working at the voxel level, lesion and tissue labels are estimated through a MRF segmentation framework that leverages spatial prior probabilities for 9 healthy tissues through multi-atlas fusion ($MALF$). This initial segmentation builds healthy and lesion intensity distributions, which are then fed to a RF (Breiman, 2001) classifier for training. The trained RF classifier provides lesion refinement at the region level.

The authors of (Shiee et al., 2010), exploit an extension of the TOpology-preserving Anatomical Segmentation ($TOADS$) algorithm (Bazin and Pham, 2008). $TOADS$ incorporates statistical and topological atlases to give a topologically consistent segmentation of healthy brain anatomy. Initially, the atlases are registered with the MRI data. Then, the method builds upon previous work (Bazin and Pham, 2008) by using the aforementioned segmentation and handling MS lesions as topological outliers. Finally, taking into account the

intensity profile of the lesions, a post-processing step for reducing false positives is applied.

3.2.1.1.4. Statistical Methodologies

Authors in (Ghafoorian and Platel, 2015) utilize a deep Convolutional Neural Network (CNN) with five layers to create a statistical voxel-based classifier. Initially, the image intensity is normalized. The CNN learns if the central voxel of a given region of interest is a lesion or not. A leave-one-out cross validation is employed to provide training data for the CNN. Stochastic gradient descent is used for the network optimization.

In (McKinley et al., 2016), a deep convolutional architecture for MS lesion segmentation is presented. The aforementioned, is a probabilistic architecture which combines a fully-convolutional network for local data information, as well as an encoder-decoder network in which convolutional layers compute high-level information. In total, 18 network layers are used.

Similar to (McKinley et al., 2016), (Brosch et al., 2016) also employs deep $3D$ convolutional encoder networks. The main idea is to segment MS lesions by finding a function that maps multimodal MRI data to corresponding binary lesion masks. The network is made up of convolutional and pooling layers. The convolutional layers are used to increase learning of more abstract and higher-level image information. The pooling layers aim to predict the final segmentation probability at the voxel level.

After performing NL-Means based denoising (Coupé et al., 2008), rigid registration (Commowick et al., 2012), skull stripping using the $VolBrain$ platform (Manjón and Coupé, 2016), inhomogeneity correction using the $N4$ algorithm (Tustison et al., 2010) and normalization on the initial MRI data, the method of (Valverde et al., 2016) proposes a CNN trained with $3D$ patches of candidate lesion voxels. The proposed CNN uses two dense convolution layers to probabilistically classify the voxels. An extension of the previous work is presented in (Valverde et al., 2017). In (Valverde et al., 2017) the CNN is improved to

a more sensitive cascaded $3D\ CNN$ which can be sufficiently trained using a small set of labeled data.

In (Doyle et al., 2018; Subbanna et al., 2015) $IMaGe$ is introduced, an Iterative Multilevel probabilistic Graphical model for the detection and segmentation of MS lesions. It includes two MRF levels. At the bottom level, a regular grid voxel-based MRF identifies potential lesion voxels, as well as other tissue classes, using local and neighborhood intensities and class priors. Contiguous voxels of a particular tissue type are grouped into regions. A higher, non-lattice MRF is then constructed, in which each node corresponds to a region, and edges are defined based on neighborhood relationships between regions. The goal of this MRF is to evaluate the probability of candidate lesions, based on group intensity, texture and neighborhood regions. The inferred information is then propagated to the voxel-level MRF which performs voxel wise classification.

Roy et al. Roy et al. (2018) applies a preprocessing step containing registration (Avants et al., 2011), skull stripping (Carass et al., 2011; Roy et al., 2017b) and $N4$ intensity inhomogeneity (Tustison et al., 2010). Then a CNN, implementing a 2 level convolution pathway is implemented. The results of the two levels are concatenated towards achieving the lesion segmentation.

Meier et al. (Meier et al., 2017) performs $N4$ intensity inhomogeneity (Tustison et al., 2010) on the initial data, followed by a coregistration (Johnson et al., 2007) and skull stripping process (Smith, 2002). Then, tissue segmentation into the three main tissue classes (WM, GM, CSF) takes place using FREESURFER tool (Fischl et al., 2002). The latter segmentation is exploited in generating individual tissue probability maps for the spatial distribution of each tissue type. The latter allows the deployment of heuristic topological-based rules. The aforementioned info is exploited by the MRF-based classification algorithm presented in (Van Leemput et al., 2001) in order to propose the lesion segmentation. A lesion size-based post-processing step for minimizing false positives integrates the proposed pipeline.

3.2.1.2. 2D Image-based Methodologies.

3.2.1.2.1. Feature-based Methodologies

The method presented in (Santos et al., 2016), initially performs inhomogeneities' correction using the $N3$ procedure (Sled et al., 1998). In the sequel, brain extraction via the *bet*2 tool (Jenkinson et al., 2005) takes place. Denoising all images with a Gaussian filter completes the pre-processing steps. A simple Multilayer Perceptron (MLP) classifier with a single hidden layer containing just a few neurons for fast computation of outputs is implemented. The classifier is trained using T2-FLAIR intensity-based features. In the post-processing stage, a lesion probability atlas (Mazziotta et al., 2001) to remove false positives occurring in low probability regions, was employed.

Andermatt et al. (Andermatt et al., 2018), uses a weighted variation of the multi-dimensional gated recurrent units ($MD-GRU$) on automated lesion segmentation in multiple sclerosis presented in (Andermatt et al., 2016). $MD-GRU$ is actually a convolution-based feature extraction model. The aforementioned model is implemented upon a Recurrent Neural Network (RNN). Their variation allows shorter training time. Data augmentation is also used for further improvement of the training.

3.2.1.2.2. Data-driven Methodologies

In (Storelli et al., 2016), the classification technique used is based on a region growing approach. Manual identification of lesions was employed to initialize the algorithm and manual segmentation was also used for the training and validation of the proposed method. The region growing approach is based on an intensity threshold function which was selected by maximizing the dice similarity coefficient between the manually and automatically outlined lesions. The disadvantage of this method is that it is considered semi-automatic due to the manual interventions that are contained within its pipeline.

3.2.1.2.3. Atlas-based Methodologies

Fleishman et al (Fleishman et al., 2018), perform some preprocessing containing N3 normalization (Sled et al., 1998), skull stripping (Carass et al., 2011), resampling and registration. In addition, based on the Joint intensity Fusion (JIF) algorithm, a synthetic image is created. JIF is a variation of multi-atlas label fusion ($MALF$) presented in (Wang et al., 2013). For the creation of the synthetic image, several brain atlases are used. The synthetic image, along with the processed data is passed through $OASIS$ classifiers in order for the lesions to be segmented.

3.2.1.2.4. Statistical Methodologies

In (Havaei et al., 2016), a typical CNN architecture which takes a multi-plane image as input, is implemented. The CNN consists of the back end, the abstraction and the front end layers. The back end uses two individual convolutional layers which create information maps based on the multimodal input. The statistics of the aforementioned maps are computed in the abstraction layer which, after concatenation, are processed by two further convolutional layers in the front end, yielding pixel-wise probabilistic classifications outputs.

3.2.2. Unsupervised Methodologies

3.2.2.1. 3D Volume-Based Methodologies.

3.2.2.1.1. Lesion-Based Methodologies

The authors of (Tomas-Fernandez and Warfield, 2015) were inspired by the ability of experts to detect lesions based on their local signal intensity characteristics. Initially, MRI data are processed to compensate for the effect of intensity inhomogeneity as well as for thermal noise. Then, an algorithm is proposed that achieves lesion and brain tissue clustering using a mixture model

for each of them. Their approach is called MOdel of Population and Subject ($MOPS$) intensities. The work in (Tomas-Fernandez and Warfield, 2016) is a different version of (Tomas-Fernandez and Warfield, 2015). After smoothing the effect of intensity inhomogeneity and thermal noise, an algorithm is proposed that achieves lesion and brain tissue clustering using a Gaussian Mixture Model (GMM) for each of them.

Based on the hypothesis that the T2-FLAIR intensity is higher in a lesion than in the surrounding region, the authors of (Urien et al., 2016), employ a max-tree representation of the MRI images (Salembier et al., 1998) which highlights regions of high relative intensity. The suspicious regions correspond to the nodes that cover two criteria. The first is based on the difference in intensities between a candidate lesion and its surroundings and the second is based on the fact that lesions tend to appear near the ventricles. To improve segmentation performance, additional constraints are used, depending on the location of the lesions with respect to more brain structures such as WM.

In (Koley et al., 2016), the normalized cross-correlation coefficient is computed as a similarity metric between $3D$ Gaussian templates with varying radii and the MRI volume. The value of the similarity metric is used to detect brain lesions. The advantage of this method is that it performs fast computation of similarity between the templates and the actual volume.

3.2.2.1.2. Tissue-Based Methodologies

In (Catanese et al., 2015), the Expectation-Maximization (EM) algorithm (García-Lorenzo et al., 2011) is used in order to cluster the brain data into WM, GM and CSF. Next, the graph-cut technique (García-Lorenzo et al., 2009) is applied to detect lesions as outliers on the aforementioned segmented tissues. Finally, a post-processing step is applied in order to help remove false positives. This step uses a fuzzy logic approach in order to estimate the WM. The MS lesions are assumed to appear surrounded by WM. Any candidate lesions that violate this criterion are removed. Finally, all candidate lesions smaller than

$3mm^3$ are discarded.

The method of (Beaumont et al., 2016b) is quite similar to (Catanese et al., 2015). At first, the MRI data are denoised with the NL-Means algorithm (Coupé et al., 2008), rigidly registered (Commowick et al., 2012), brain extracted using the $VolBrain$ platform (Manjón and Coupé, 2016) and bias corrected using the $N4$ algorithm (Tustison et al., 2010). Next, the EM algorithm (García-Lorenzo et al., 2011) is used for brain tissue clustering. The results initialize the graph-cut approach (García-Lorenzo et al., 2009) which detects lesions as outliers. Finally, the application of rules to remove false positives takes place.

Initially, the method presented in (Beaumont et al., 2016a) performs registration and intensity normalization on the MRI data. Then, a modification of the Maximum Likelihood Estimator (MLE) (Notsu et al., 2014) in order to cluster the brain structures into CSF, WM and GM is used. MS lesions are considered as outliers of the aforementioned model. Finally, the segmentation is refined by applying several lesion appearance rules.

In method (Roura et al., 2016) image denoising, using the anisotropic diffusion filter of (Perona and Malik, 1990), is initially applied on the MRI data. Then, the $N3$ normalization method (Sled et al., 1998) for inhomogeneities' correction is used. Next, skull stripping and tissue clustering, using the algorithm of (Ashburner and Friston, 2005) is performed. As a result, each voxel is characterized as WM, GM or CSF. MS lesions are segmented as outliers to the normal tissue. Finally, a false positive reduction step, based on discarding lesions forming elongated shapes, is applied.

The $SPM8$ (`http://www.fil.ion.ucl.ac.uk/spm`) and its $VBM8$ toolbox (`http://dbm.neuro.uni-jena.de/vbm`) is used by method (Schmidt et al., 2012) as a pre-processing step. Next, the three tissue classes of GM, WM and CSF are determined. Then, the T2-FLAIR intensity distribution of each tissue class is recruited in order to detect outliers, which are interpreted as lesion beliefs. Finally, neighboring voxels are analyzed and assigned to lesions through a lesion growth model. This is done iteratively until no further voxels are assigned

to lesions, thus resulting in a final lesion map.

The authors of (Doyle et al., 2016) initially perform registration and inhomogeneities correction using the $N4$ algorithm (Tustison et al., 2010). Then, a weighted Gaussian tissue model is used to perform a first clustering of the brain tissues into the three main clusters (CSF, WM and GM). Outlier voxels that are not well described by the normal tissue model, are characterized as lesion candidates. The candidate lesion regions are used to populate the weighted Gaussian model and guide convergence to an optimal solution.

In (Roura et al., 2015) the segmentation process is initiated by a pre-processing step including skull stripping (Smith, 2002), denoising, $N3$ inhomogeneities' correction (Sled et al., 1998) and intra-subject co-registration. Then, the $SPM8$ tissue segmentation algorithm (Ashburner and Friston, 2005) is used for segmenting normal brain WM, GM and CSF tissues. A linear combination of the mean and the standard deviation of the GM intensity distribution is used as a threshold to detect outliers which constitute the set of candidate lesions. Finally, further filtering, involving the neighborhood and the size of the candidate lesions, is utilized in order to neglect false positives.

3.2.2.1.3. Atlas-Based Methodologies

The technique presented in (Freire and Ferrari, 2016) begins with a very rich pre-processing procedure which involves noise reduction (Buades et al., 2005), inhomogeneity correction (Tustison et al., 2010) and image registration using the $NiftyReg$ tool (`http://sourceforge.net/projects/niftyreg/`). Then, three probabilistic anatomical atlases, corresponding to GM, WM and CSF, obtained by (Mazziotta et al., 2001), are recruited. These atlases are used for intensity-based clustering of the brain using the proposed iterative Student's t mixture algorithm. This algorithm continuously refines the resulting segmented tissue subclasses until all MS lesions are grouped as one simple class. Finally, a post-processing step is applied in order to remove false positives.

Dong et al. (Dong et al., 2017), uses a JIF approach similar to (Fleishman

et al., 2018). They recruit different brain atlases than (Fleishman et al., 2018). In addition, they do not use the $OASIS$ classifier. Instead, they use the Joint Label Framework (JLF) (Wang et al., 2013) where the total segmentation error is expressed as pairwise expected joint segmentation errors for all pairs of atlases used.

3.2.2.2. 2D Image-Based Methodologies.

3.2.2.2.1. Lesion-Based Methodologies

In (Knight and Khademi, 2016), MRI data is corrected in terms of intensity inhomogeneity using the $SPM12$ toolbox (Ashburner and Friston, 2005). A $3D$ Gaussian low-pass filter is then used to minimize random noise. Next, fuzzy clustering using an edge-based model (Khademi et al., 2012, 2014) is performed. This model assumes that the gray levels of each tissue cluster are distributed along a unique range. The initial fuzzy clustering is thresholded to give a binary segmentation image. Finally, false positive reduction strategies are appended to the pipeline to refine the segmentation; these strategies involve brain volume and distance metrics.

After performing skull-stripping (Smith, 2002) and inhomogeneities' correction (Tustison et al., 2010), method presented in (Weiss et al., 2013) extracts and normalizes $2D$ image patches of the initial MRI data. The $2D$ patches are used for the creation of a dictionary which defines normal tissues. Based on the aforementioned dictionary, an error map is constructed for each patch highlighting lesions as errors. Finally, a thresholding technique is applied on the error maps in order to only keep the lesions.

Initially, authors in (Roy et al., 2017a), use a skull removal methodology (Roy et al., 2016) to improve MS lesion segmentation. Then, the method is composed of two key steps: background generation and binarization. In the first step, the contour of the brain is exploited in order to create an adaptive background image. This image consists of normal tissues without any MS lesions. In the

second step, a binarized method that selects a threshold based on entropy and standard deviation (Roy et al., 2013) is used. This step derives a binarized image consisting of MS lesion and other normal tissues. The background image is then subtracted from the binarized image to segment out the MS lesions.

3.2.2.2.2. Tissue-Based Methodologies

In (Hill et al., 2015), the initial MRI data is skull-stripped, rescaled and histogram manipulated. Then, the multi-contrast data is mapped to pseudo-color images. Next, the Improved Jump Method (IJM) (Sugar and James, 2003) is used for clustering CSF, WM and GM structures. IJM is enhanced by the Canny edge detector (Ding and Goshtasby, 2001), in order to outline edges with low error and thus further improve clustering performance. From this preliminary clustering, a pseudo-color to gray-scale conversion is designed to equalize the intensities of the normal brain tissues, leaving the MS lesions as outliers.

3.2.2.2.3. Data-driven Methodologies

The authors of (Rodrigo et al., 2013), initially automatically locate hyperintense pixels on the T2-FLAIR MRI images using dynamic threshold binarization. These pixels are considered to be the centroids of lesion areas. The aforementioned hyperintensity pixels are used as seed points for an intensity-based region growing approach. The latter aims to extend the areas around the seed points until MS lesion areas are distinguished.

The first step of method (Ali and Maher, 2016) is to perform skull stripping on the initial MRI data. Then, it performs lesion segmentation by utilizing a second order differentiation approach. The main target of such an approach is to detect structure edges on the brain data. They include a smoothing process (i.e. using a $2D$ Gaussian operator) followed by the second order derivative (i.e. Laplacian differential operator) to differentiate between image regions. To this

end, (Ali and Maher, 2016) adopts the Marr-Hildreth edge detector (Marr and Hildreth, 1980).

(Keeli et al., 2017) also performs skull stripping as a first pre-processing step. Then, in order to improve the sensitivity of lesion detection, a series of further operations are applied to the image obtained from the skull stripping step. First, Local Histogram Equalization (LHE) (Boudraa et al., 2000) is applied on the brain tissue. Then, pixels of the pre-processed image are clustered using the fuzzy C means clustering algorithm (Bezdek, 1973). The intensity values of the pixels are used in order to feed the clustering process. To complete lesion detection a region-growing algorithm (Yu and Yla-Jaaski, 1991) is employed, which enables the determination of the exact boundaries of lesions. Finally, GPU-accelerated volumetric calculation and $3D$ model construction are performed to provide a $3D$ segmentation.

4. Comparison of reviewed methods

An extensive set of aspects of the reviewed methodologies are compared in the form of tables. This leads to useful conclusions discussed in Section 5. Note that the techniques reviewed in the current survey represent the state-of-the-art of methodologies published since 2013. Table 5 gives the main comparison of the methodologies reviewed. Each method is analyzed according to the database used for its experiments, the MRI image sequences used, the MRI slice thickness (in millimeters), the data handling category, its main algorithmic strategy, whether it is supervised or not, the classifier or clustering method it uses, its computational efficiency and, finally, its performance. The computational efficiency is related to the mathematical approach used and is thus deduced from Table 7. For the most cases the performance is expressed in terms of the mean DSC measure which is the most common among all methodologies. Only for the cases of the techniques tested on $MICCAI$ 2008 data set, the performance is expressed by an overall score combing the VD, SEN and $FALL$ metric (see Section 2). Methodologies tested on the same database are much more reliably

compared. Some methodologies are tested on more than one databases. Figures 5, 6, 7 and 8 illustrate the performance of the state-of-the-art methodologies tested on the same database ($MICCAI$ 2008, $ISBI$ 2015 and $MICCAI$ 2016 respectively). Taking into account methodologies (Brosch et al., 2016; Geremia et al., 2013; Havaei et al., 2016) and (Hill et al., 2015; Shiee et al., 2010) which were tested on the same database ($MICCAI$ 2008 and $BrainWeb$ respectively), the ones published after 2013 are quite comparable to the earlier ones in terms of performance.

Table 6 records the advantages and disadvantages of each proposed category, while Table 7 presents the characteristics of the mathematical approaches implemented by the reviewed methodologies in their main strategy. Table 8 illustrates the popularity of each category. Finally, Table 9 shows the advantageous characteristics of each MRI acquired image sequence over the MS lesion segmentation problem.

METHOD	DATABASE	*MRI* DATA	*MRI* SLICE THICKNESS	*MRI* SLICE GAP	DATA HANDLING	STRATEGY	SUPEVISION	CLASSIFIER	CLUSTERING	COMPUTATIONAL EFFICIENCY	PERFORMANCE (DSC)
(McKinley et al., 2016)	*MICCAI* 2016	T2-FLAIR	0.0 mm	No gap	*3D* Volume	Statistical	YES	*CNN*	NO	Low	0.591
(Roura et al., 2016)	*MICCAI* 2016	T1-w, T1-w *Gd*, T2-FLAIR	1.0 mm	No gap	*3D* Volume	Tissue-based	NO	NO	*GMM*	Medium	0.572
(Valverde et al., 2016)	*MICCAI* 2016	T1-w, T1-w *Gd*, T2-w, T2-FLAIR, *PD-w*	1.0 mm	No gap	*3D* Volume	Statistical	YES	*CNN*	NO	Low	0.541
(Vera-Olmos et al., 2016)	*MICCAI* 2016	T1-w, T1-w *Gd*, T2-FLAIR	1.0 mm	No gap	*3D* Volume	Statistical	YES	*MRF*	NO	Medium	0.521
(Knight and Khademi, 2016)	*MICCAI* 2016	T2-FLAIR	1.0 mm	No gap	*2D* Images	Lesion-based	NO	NO	NO	High	0.490
(Doyle et al., 2016)	*MICCAI* 2016	T1-w, T1-w *Gd* T2-FLAIR	1.0 mm	No gap	*3D* Volume	Tissue-based	NO	NO	*GMM*	Medium	0.489
(Beaumont et al., 2016a)	*MICCAI* 2016	T2-w, T2-FLAIR	1.0 mm	No gap	*3D* Volume	Tissue-based	NO	NO	*MLE*	Medium	0.485
(Beaumont et al., 2016b)	*MICCAI* 2016	T1-w, T1-w *Gd*, T2-w, T2-FLAIR, *PD-w*	1.0 mm	No gap	*3D* Volume	Tissue-based	NO	NO	*EM*	Medium	0.453
(Mahbod et al., 2016)	*MICCAI* 2016	T1-w, T1-w *Gd*, T2-w, T2-FLAIR, *PD-w*	1.0 mm	No gap	*3D* Volume	Statistical	YES	*ANN*	NO	Low	0.430
(Urien et al., 2016)	*MICCAI* 2016	T1-w, T1-w *Gd*, T2-w, T2-FLAIR, *PD-w*	1.0 mm	No gap	*3D* Volume	Lesion-based	NO	NO	NO	High	0.347
(Muschelli et al., 2016)	*MICCAI* 2016	T1-w, T1-w *Gd*, T2-w, T2-FLAIR, *PD-w*	1.0 mm	No gap	*3D* Volume	Statistical	YES	*RF*	NO	Medium	0.341
(Santos et al., 2016)	*MICCAI* 2016	T1-w, T1-w *Gd*, T2-w, T2-FLAIR, *PD-w*	1.0 mm	No gap	*2D* Images	Data-driven	YES	*MLP*	NO	Medium	0.340
(Tomas-Fernandez and Warfield, 2016)	*MICCAI* 2016	T1-w, T1-w *Gd*, T2-w, T2-FLAIR	1.0 mm	No gap	*3D* Volume	Lesion-based	NO	NO	*GMM*	Medium	0.228
(Freire and Ferrari, 2016)	*ISBI* 2015	T1-w, T2-w, T2-FLAIR, *PD-w*	2.2 mm	N/A	*3D* Volume	Atlas-based	NO	NO	Atlas	High	0.659
(Jesson and Arbel, 2015)	*ISBI* 2015	T1-w, T2-w, T2-FLAIR	2.2 mm	N/A	*3D* Volume	Atlas-based	YES	*RF*	NO	Medium	0.638
(Andermatt et al., 2018)	*ISBI* 2015	T1-w, T2-w, T2-FLAIR, *PD-w*	2.2 mm	N/A	*2D* Images	Fouture-based	YES	*RNN*	NO	Low	0.629
(Ghafoorian and Platel, 2015)	*ISBI* 2015	T1-w, T2-w, T2-FLAIR, *PD-w*	2.2 mm	N/A	*3D* Volume	Statistical	YES	*CNN*	NO	Low	0.614
(Maier and Handels, 2015)	*ISBI* 2015	T1-w, T2-w, T2-FLAIR, *PD-w*	2.2 mm	N/A	*3D* Volume	Statistical	YES	*RF*	NO	Medium	0.609
(Catanese et al., 2015)	*ISBI* 2015	T1-w, T2-w, T2-FLAIR	2.2 mm	N/A	*3D* Volume	Tissue-based	NO	NO	*EM*	Medium	0.607
(Prados et al., 2015)	*ISBI* 2015	T1-w, T2-w, T2-FLAIR, *PD-w*	2.2 mm	N/A	*3D* Volume	Data-driven	YES	*3D* Templates	NO	High	0.598
(Shiee et al., 2010)	*ISBI* 2015	T1-w, T2-FLAIR	2.2 mm	N/A	*3D* Volume	Atlas-based	YES	*3D* Templates	NO	High	0.579
(Roy et al., 2018)	*ISBI* 2015	T1-w, T2-w, T2-FLAIR	2.2 mm	N/A	*3D* Volume	Statistical	YES	*CNN*	NO	Low	0.524
(Joq et al., 2015)	*ISBI* 2015	T1-w, T2-w, T2-FLAIR	2.2 mm	N/A	*3D* Volume	Data-driven	YES	Decision Trees	NO	Low	0.474
(Iheme and Unay, 2015)	*ISBI* 2015	T2-FLAIR	2.2 mm	N/A	*3D* Volume	Data-driven	YES	Threshold-based	NO	Low	0.426
(Tomas-Fernandez and Warfield, 2015)	*ISBI* 2015	T1-w, T2-w, T2-FLAIR	2.2 mm	N/A	*3D* Volume	Lesion-based	NO	NO	*GMM*	Medium	0.415
(Valverde et al., 2017)	*MICCAI* 2008	T1-w, T2-w, T2-FLAIR	0.5 mm	No gap	*3D* Volume	Statistical	YES	*CNN*	NO	Low	0.871
(Guizard et al., 2015)	*MICCAI* 2008	T1-w, T2-w, T2-FLAIR	0.5 mm	No gap	*3D* Volume	Data-driven	YES	*3D* Templates	NO	High	0.861
(Tomas-Fernandez and Warfield, 2015)	*MICCAI* 2008	T1-w, T2-w, T2-FLAIR	0.5 mm	No gap	*3D* Volume	Lesion-based	NO	NO	*GMM*	Medium	0.844
(Brosch et al., 2016)	*MICCAI* 2008	T1-w, T2-w, T2-FLAIR	0.5 mm	No gap	*3D* Volume	Statistical	YES	*CNN*	NO	Low	0.840
(Strumia et al., 2016)	*MICCAI* 2008	T1-w, T2-FLAIR	0.5 mm	No gap	*3D* Volume	Data-driven	YES	*3D* Templates	*GMM*	Medium	0.839
(Havaei et al., 2016)	*MICCAI* 2008	T1-w, T2-w, T2-FLAIR	0.5 mm	No gap	*2D* Images	Statistical	YES	*CNN*	NO	Low	0.832
(Roura et al., 2015)	*MICCAI* 2008	T1-w, T2-FLAIR	0.5 mm	No gap	*3D* Volume	Tissue-based	NO	NO	NO	High	0.823
(Geremia et al., 2013)	*MICCAI* 2008	T1-w, T2-w, T2-FLAIR	0.5 mm	No gap	*3D* Volume	Data-driven	YES	*RF*	NO	Medium	0.821
(Shiee et al., 2010)	*MICCAI* 2008	T1-w, T2-FLAIR	0.5 mm	No gap	*3D* Volume	Atlas-based	YES	*3D* Templates	NO	High	0.799
(Shiee et al., 2010)	*BrainWeb*	T1-w, T2-w, *PD-w*	2.2 mm	N/A	*3D* Volume	Atlas-based	YES	*3D* Templates	NO	High	0.789
(Hill et al., 2015)	*BrainWeb*	T1-w, T2-w, *PD-w*	N/A	N/A	*2D* Images	Tissue-based	NO	NO	*1JM*	Low	0.739
(Weiss et al., 2013)	*BrainWeb*	T1-w, T2-w	1.0 mm	N/A	*2D* Images	Data-driven	NO	NO	NO	High	0.710
(Roy et al., 2017a)	*WholeBrainAtlas*	T1-w, T2-w, *PD-w*	0.5 mm	1.0 mm	*2D* Images	Tissue-based	NO	NO	NO	High	N/A
(Keeli et al., 2017)	Proprietary	T2-FLAIR	N/A	N/A	*2D* Images	Data-driven	NO	NO	Fuzzy *C* Means	Medium	0.841
(Schmidt et al., 2012)	Proprietary	T1-w, T2-FLAIR	1.0 mm	No gap	*3D* Volume	Tissue-based	NO	NO	NO	High	0.753
(Steenwijk et al., 2013)	Proprietary	T1-w	1.0 mm	No gap	*3D* Volume	Atlas-based	YES	$k-NN$	NO	Low	0.740
(Subbanna et al., 2015)	Proprietary	T1-w, T2-w, T2-FLAIR, *PD-w*	N/A	N/A	*3D* Volume	Statistical	YES	*MRF*	NO	Medium	0.690
(Storelli et al., 2016)	Proprietary	T2-w, *PD-w*	3.0 mm	N/A	*2D* Images	Data-driven	YES	Threshold-based	Region Growing	Low	0.620
(Dong et al., 2017)	Proprietary	T1-w, T2-FLAIR	N/A	N/A	*3D* Volume	Atlas-based	YES	*JLF*	NO	High	0.586
(Fleishman et al., 2018)	Proprietary	T1-w, T2-w, T2-FLAIR, *PD-w*	N/A	N/A	*2D* Images	Atlas-based	YES	*OASIS*	NO	High	0.570
(Meier et al., 2017)	Proprietary	T1-w, T2-w, T2-FLAIR	1.0 mm	N/A	*3D* Volume	Statistical	YES	*MRF*	FREESURFER	Low	0.510
(Koley et al., 2016)	Proprietary	T2-w, T2-FLAIR	1.0 mm	N/A	*3D* Volume	Lesion-based	NO	NO	*3D* Templates	High	N/A
(Rodrigo et al., 2013)	Proprietary	T2-w, T2-FLAIR, *PD-w*	N/A	N/A	*2D* Images	Data-driven	NO	NO	Region Growing	High	N/A
(Ali and Maher, 2016)	Proprietary	T2-w	N/A	N/A	*2D* Images	Data-driven	NO	NO	Threshold-based	Low	N/A

Table 5: Comparison of MS lesion segmentation methodologies since 2013.

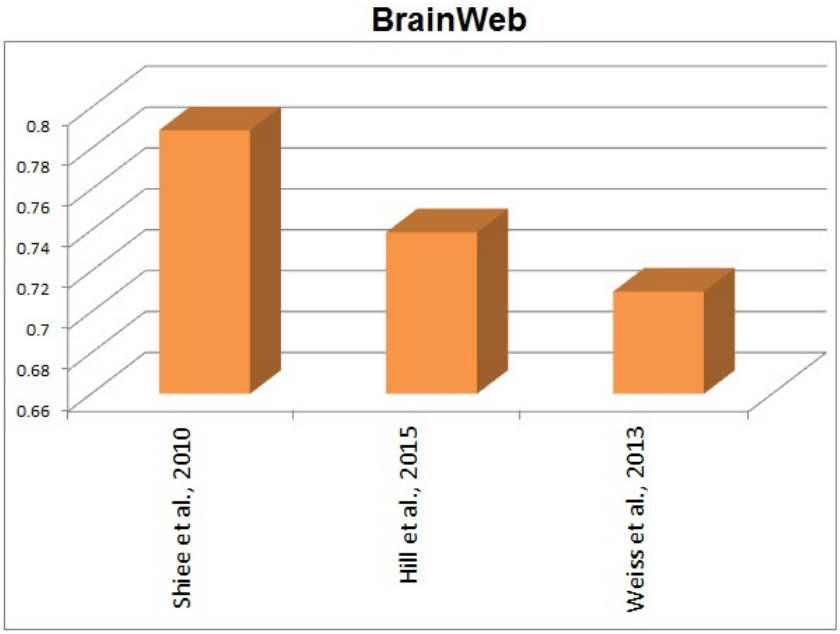

Figure 5: Performance of the state-of-the-art techniques tested on *BrainWeb* synthetic database.

5. Discussion

MRI is the most widely used imaging modality for diagnosing and following up the *MS* disease. *MS* is manifested through lesions in the brain which are usually asymmetric. The number and size of these lesions are important signs of the progression of the disease.

Regarding the modalities, T1-w images are widely used for the tissue segmentation and in this modality lesions appear as hypointensities. *MS* lesions are usually detected in the T2-w and *PD*-w modalities where they appear as hyperintensities. The major drawback of these images is the similarity in the intensities of lesions and *CSF*, which makes the discrimination between ventricles and lesions difficult, especially when they are connected. In such cases, T2-FLAIR images can be of great importance, but such images have problems

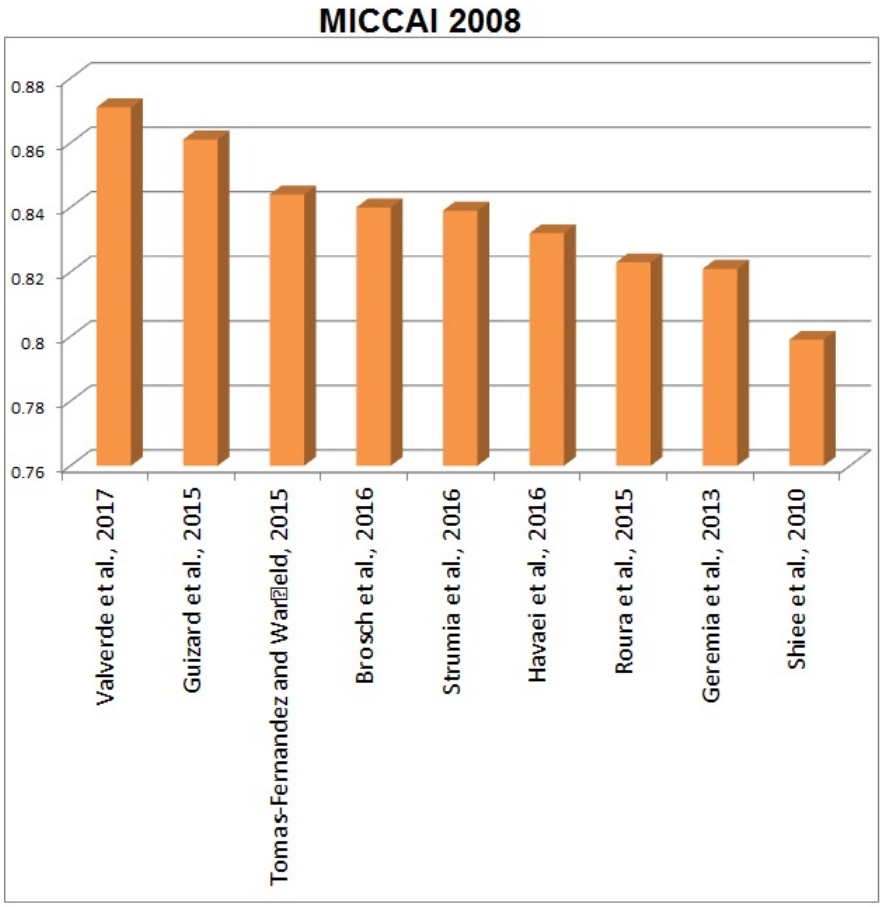

Figure 6: Performance of the state-of-the-art techniques tested on $MICCAI$ 2008 database.

when dealing with sub-cortical structures. One could therefore conclude that there is great promise in multi-modal MS lesion segmentation techniques. The pros and cons of the various modalities are presented in Table 9.

The evaluation and comparison of MS lesion segmentation techniques present difficulties as there are only a few public databases, with corresponding ground truth, that can be used as evaluation benchmarks (see Table 2). In addition, the aforementioned databases contain a small number of subjects. Issues of the results' reproducibility from these databases thus arise. Furthermore, these databases are not suitable for recruiting powerful state-of-the-art machine learn-

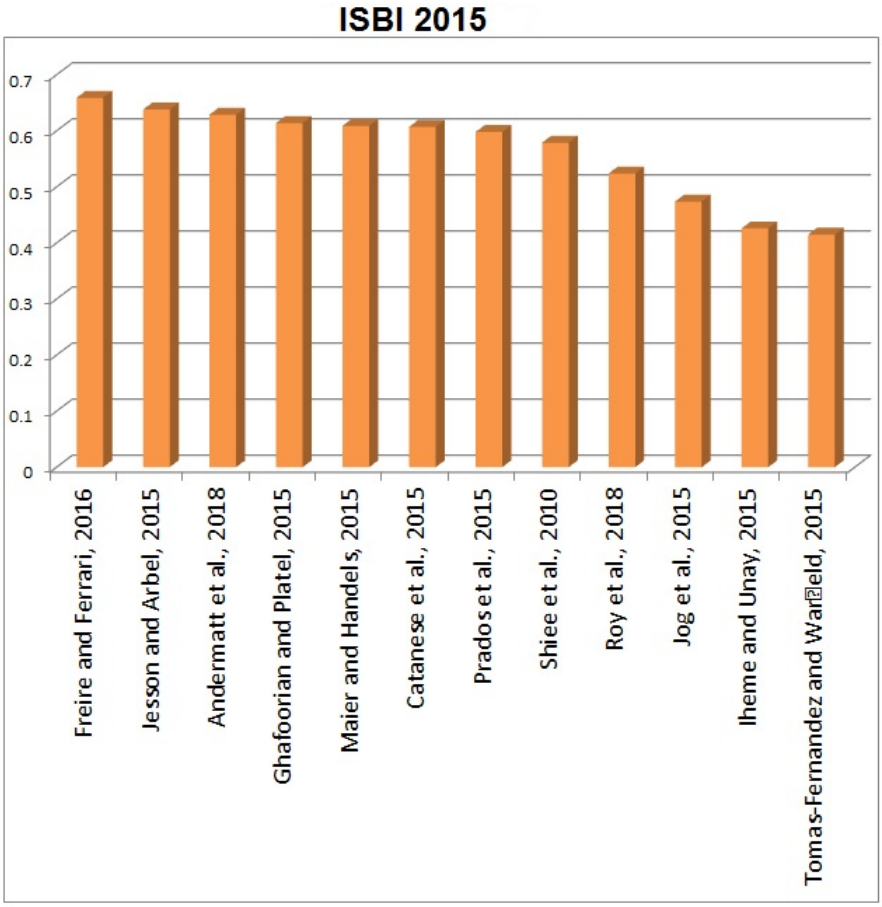

Figure 7: Performance of the state-of-the-art techniques tested on $ISBI$ 2015 database.

ing techniques, due to the restricted number of subjects contained. Consequently, there is a need for large-scale public benchmark databases with ground truth. The idea of creating synthetic big databases based on small real ones seems to be very appealing on that matter.

The criteria used in order to quantify the performance of MS lesion segmentation methodologies (see Table 3) can be classified into 5 groups. The deterministic, the probabilistic, the area, the volume and the distance one (see Table 4). The most popular group is the deterministic one, where each voxel is assigned to only one tissue type, while the most common measure is the

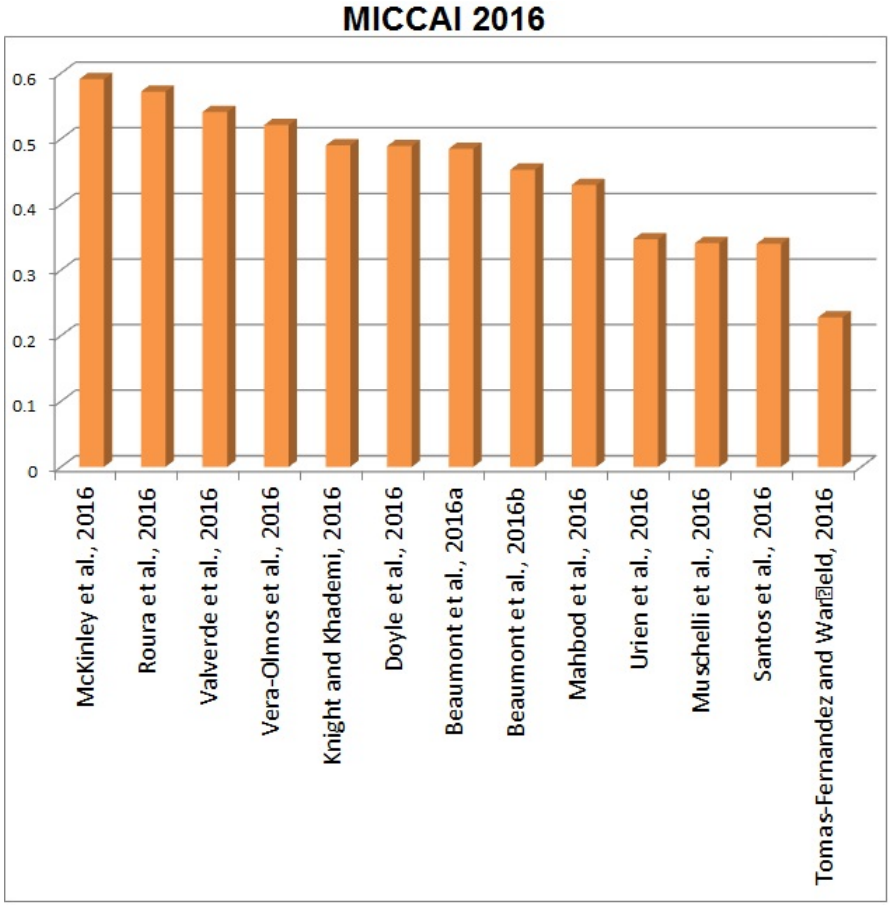

Figure 8: Performance of the state-of-the-art techniques tested on $MICCAI$ 2016 database.

DSC. However, different types of measures should be combined to obtain a more objective and reliable assessment (Cárdenes et al., 2009).

We have categorized the methodologies of the state-of-the-art based on how they handle their input, their main strategy and on their supervision type. As far as the handling of the input is concerned, 2 sub-categories are suggested: $3D$ volume-based and $2D$ image sequence-based. The first sub-category contains 33 methodologies while the second only 12. Using $3D$ metrics for disease interpretation, such as volumetry and $3D$ voxel neighborhood, most of the times outperforms the, easier to handle, $2D$ data.

CATEGORY	ADVANTAGES	DISADVANTAGES
Supervised	1. A wide list of classifiers can be used 2. Strengthen accuracy due to training process	1. Time consuming due to training process
Unsupervised	1. Fast set up as no training process needed	1. Wrong assumption of normal distributions for the intensity of brain tissues 2. More difficult to achieve high accuracy
$3D$ volume-based	1. $3D$ voxels' neighborhood can be considered 2. Direct $3D$ MS lesion segmentation is implied	1. Time consuming calculations when large voxels' neighborhood are taken into account
$2D$ image sequence-based	1. Easier to processing than $3D$ volumes 2. Faster operators can be exploited	1. Only $2D$ voxels' neighborhood can be considered 2. $3D$ volume reconstruction needed to provide $3D$ MS lesion segmentation
Atlas-based	1. Local information included 2. Segmented structures are spatially constrained	1. Registration needed 2. Previous segmentations for atlas creation needed
Data-driven	1. Simple to implement	1. Relatively inaccurate
Statistical	1. Balance between performance and implementation	1. Time consuming calculations needed
Tissue-based	1. Lesion segmentation is smoothly guided	1. Quality of the tissue segmentation dependance
Lesion-based	1. Sub-lesions can be segmented	1. Artifacts may share lesion properties

Table 6: Advantages and disadvantages of each category of MS lesion segmentation methodologies.

In terms of their main strategy, 6 sub-categories are suggested: the atlas-based, the statistical, the lesion-based, the data-driven, the tissue-based and the feature-based. The first sub-category, which is the least popular one, contains 5 methods, the second contains 9 and the third contains 6 methods, the fourth has 7 methods, the fifth includes 8 methods and the final sub-category is the most popular one counting 10 methods. The most recently appeared methods are statistical and are mainly based on convolutional neural networks (CNN). Thus, it appears that CNN is a trend on the field. However, based on the results of the challenges, it is clear that further wok is needed for CNNs to get to their full potential.

Finally, based on the segmentation approach, 2 sub-categories are suggested: supervised and unsupervised methods. The supervised and unsupervised methodologies almost share popularity containing 26 and 19 methods respectively. This result cannot indicate a trend towards supervised or unsupervised direction. The fact that unsupervised methods avoid the time-consuming training process, which needs the acquisition of a respectable amount of data, may be a reason for choosing an unsupervised strategy. On the other hand, exploiting the powerful properties of the classifiers, especially of the CNN, can be a reason for choosing a supervised mentality. All the aforementioned statements are illustrated in Table 8, where the popularity of each method is expressed as

MODEL	ACCURACY	TIME-COMPLEXITY	SPACE-COMPLEXITY
CNN	High	High	High
RF	High	Medium	Medium
$k-NN$	Medium	High	High
ANN	Medium	High	High
Decision Trees	Medium	High	Medium
MLP	Medium	Medium	Medium
Threshold-based	Low	High	Low
IJM	High	High	Medium
CRF	High	Medium	Medium
Max-Tree	Medium	Medium	Medium
GMM	Medium	Medium	Medium
Fuzzy C Means	Medium	Medium	Low
MRF	Medium	Medium	Low
EM	Medium	Medium	Low
MLE	Medium	Medium	Low
Region Growing	Low	Low	Low

Table 7: Characteristics of the mathematical approaches implemented by the MS lesion segmentation methodologies.

percentage units.

Some useful conclusions can be extracted from Figure 2. First, there are no unsupervised feature-based and statistical methodologies. This is because feature-based techniques implement their extracted features to provide input to some sort of training process, while most statistical methodologies employ CNNs, which involve supervised training, thus, they cannot be unsupervised. Second, there are no supervised tissue or lesion-based methods. This is because the logical path for unsupervised techniques which do not have any prior knowledge, is to simulate the clinical procedure, based on clinical knowledge which is expressed computationally and relates the MRI data to the brain anatomies, in order to segment these anatomies (including lesions). Third, due to the fact that the most popular brain atlases are $3D$, there is only one atlas-based method-

CATEGORY	POPULARITY (%)	CATEGORY	POPULARITY (%)	CATEGORY	POPULARITY (%)
Supervised	58	$3D$ Volume-based	51	Atlas-based	4
				Data-driven	8
				Feature-based	20
				Statistical	19
		$2D$ Image sequences-based	7	Atlas-based	1
				Data-driven	2
				Feature-based	2
				Statistical	2
Unsupervised	42	$3D$ Volume-based	28	Atlas-based	4
				Data-driven	0
				Tissue-based	16
				Lesion-based	8
		$2D$ Image sequences-based	14	Atlas-based	0
				Data-driven	6
				Tissue-based	2
				Lesion-based	6

Table 8: Category popularity of MS lesion segmentation methodologies (number of methodologies).

ology using MRI data exclusively as $2D$ image sequences. Finally, there are no unsupervised $3D$ volume-based data-driven methodologies. This may lie to the fact that most of the data-driven algorithms, which are used mainly for clustering in the case of unsupervised methods, operate on $2D$ data, instead of $3D$ volumes.

According to Table 6, the supervised $3D$ volume-based methods appear to have more advantages than other combinations. On the contrary, unsupervised $2D$ image sequence-based methods appear to have more disadvantages than any other combination. Thus, taking also into account the results of Table 5, when it comes to techniques tested on the same data sets, it appears that supervised $3D$ volume-based methodologies are more advantageous, as they achieve better performance. However, the performance of a methodology alone is not sufficient to decide on its appropriateness in real world applications. Computational efficiency is also important in real-world applications and this is indicated in Tables 5 and 7. Most techniques use MRI brain data having zero slice thickness, which is the most time-consuming data to capture. On the other hand, MRI zero slice thickness facilitates the imaging of the whole volume of lesions, resulting

MRI IMAGE SEQUENCE	PROPERTIES
T1-w T1-w Gd	1. MS lesions appear as hypointensities 2. Anatomical images 3. Useful for image registration
T2-w	1. MS lesions appear as hyperintensities 2. CSF, GM and MS lesions have similar intensities 3. MS lesions are better highlighted than in PD-w
PD-w	1. MS lesions appear as hyperintensities 2. MS lesions and CSF are not easily distinguished
T2-FLAIR	1. MS lesions appear as hyperintensities 2. CSF and MS lesions intensities can be distinguished 3. MS lesions placed in brain stem and cerebellum are hard to be distinguished

Table 9: Properties of MRI acquired data.

in better performance.

As Table 7 indicates, which is an enrichment of a table illustrated in (Mortazavi et al., 2012), when it comes to supervised classification, CNN and RF are the most robust approaches. Although the aforementioned approaches have high time and space complexity (especially CNN), this is outbalanced by the high achieved performance of the MS lesion segmentation techniques into which they are integrated. Space complexity is not a major issue nowadays, so long as it does not grow beyond control, e.g. exponentially. In terms of clustering, IJM and CRF are robust. However, IJM could use some acceleration. Thus there are indications that supervised MS lesion techniques which integrate CNNs or RFs and unsupervised clustering-based techniques which implement IJM or CRF are more promising.

The analysis of the previous paragraphs agrees with the conclusions extracted from Table 5. More precisely, supervised $3D$ volume-based methodologies using statistical approaches for their main strategy and a CNN or RF classifier occupy top performance places among other techniques tested on the same databases. On the other hand, data-driven techniques (whether supervised or unsupervised, $3D$ volume or $2D$ image-based) appear to achieve worse performance. This could be explained by the fact that data-driven techniques

are exclusively based on intensity and spatial features of the MRI data, which are pretty simple cues. It should be noted that, despite the progress in the field, there is not yet a specific segmentation approach which can be used as standard. This is probably because the results are still below the expert neuroradiologists' and clinical doctors' performance. For example, on the $MICCAI$ 2016 database the DSC achieved by an expert human rater is 0.782 while method (McKinley et al., 2016) achieves the highest DSC which equals to 0.591. Consequently, there is much room for further improvement here.

6. Future challenges

The first future challenge concerns MRI data acquisition. In recent years, enriched MRI protocols, such as magnetization transfer imaging, quantitative MRI, diffusion tensor imaging, and magnetic resonance spectroscopy (Bakshi et al., 2008; Blystad et al., 2016; Zivadinov et al., 2008) have been developed. Although these techniques are more complicated to implement and interpret and thus not yet widely used in clinical practice, it is expected that their continuous improvement, in terms of standardization and optimization, will establish them in the future. Combining different magnetic resonance methods, which are sensitive to different aspects of MS pathology appears to be a promising path to further improve the performance of automated MS lesion segmentation methods (Vrenken et al., 2013). In addition, using such multimodal data, future segmentation methodologies could be able to even distinguish among MS lesion sub-classes (i.e. black holes, enhancing lesions), instead of just segmenting them (Tadayon et al., 2016).

Another future challenge has to do with the injection of the contrast medium during the MRI data acquisition process. Although contrast-enhancing MS lesions is an important tool for diagnosing and monitoring MS, intravenous contrast agents involve an expense and a potential risk of adverse effects for the patients. Thus, it would be desirable to identify active lesions without using a contrast agent. Presently, it seems that Gd injection cannot be avoided (Blystad

et al., 2016), but it is expected that the automated MS lesion segmentation techniques of the future could provide solutions without it.

Comparing different automated MS lesion segmentation techniques, based on MRI data, faces objective difficulties. To begin with, not all the approaches of the-state-of-the-art are publicly available to the research community. Furthermore, many of the methodologies are tested on proprietary MRI databases, making the comparison between them unreliable. There are only a few cases where a (small) number of techniques were tested on the same database (Carass et al., 2017; Commowick et al., 2016; Styner et al., 2008). The aforementioned databases are remarkable efforts but suffer from the fact that they are very restricted in terms of the number of subjects, raising issues of reproducibility. A large scale benchmark database, along with the corresponding ground truth, would be a very positive addition to this thriving field. However, collecting many thousands of brain MRI data is not an easy task. A first work recruiting synthetic data, instead of real clinical data, is the so-called $BrainWeb$ database (Cocosco et al., 1997). However, this database still produces a very restricted number of brain MRI data.

Future brain MRI-based MS lesion segmentation techniques are expected to be hybrid. Combining the most promising individual strategies of the state-of-the-art and exploiting their combined advantages, should prove very useful in order to further improve MS lesion segmentation performance. In addition, combining the advantages of different techniques may compensate some of the missing parts of some strategies and may enable the development of less subjective and more automated approaches. Although supervised techniques presently achieve better results, it is also expected that, in the future, effort will also be directed to unsupervised techniques in order to avoid the costly training process. Finally, in a more generic framework, robust MS lesion segmentation techniques can be used for MS lesion quantification in clinically relevant settings like patients' eFolder Ma et al. (2015).

7. Conclusions

MS is a chronic disease that influences the central nervous system of the patients, affecting their daily routine. MRI is the most widely used imaging technique for diagnosing and following up MS lesions. The manual detection of MS lesions in the MRI images is a process that is time-consuming, subjective and prone to human errors. This stresses the importance of the implementation of automated MS lesion segmentation techniques, which is an open research field due to the challenges which arise from the variability of the intensity values of MS lesions in MRI images, among others.

In the current survey we provide a comprehensive review of up-to-date state-of-the-art automated MS lesion segmentation methodologies, published from 2013 onwards. In addition, the most common data sets and evaluation measures used in this field are reviewed. The aforementioned methodologies were categorized according to their technical nature. Comparing different approaches is difficult, due to the lack of a common database and a proper gold standard, but general trends can be identified and their advantages and disadvantages help pave the way for researchers who wish to improve or develop new automated methods. A detailed discussion of the reviewed works and a comparison of their performance is given. Future challenges and aspects of potential methodologies are identified.

Despite recent progress, there is not yet a specific automated lesion segmentation approach robust enough to emerge as a standard. The main reasons are the mediocre (but rapidly) improving results and the high computational cost. Thus it seems that there is room for improvement in the automated segmentation of MS lesions using MRI data. New algorithms, new advances in MRI acquisition protocols and new hardware-based differential diagnosis will undoubtedly assist neuroradiologists in improving the early diagnosis and assessment of therapies as well as the differential follow-up.

Acknowledgment

D.A. Verganelakis would like to gratefully acknwoledge the financial support by the Association of Friends of Children with Cancer ('ELPIDA').

References

Ali, S. M., Maher, A., 2016. Identifying multiple sclerosis lesions in MR images using image processing techniques. In: 2016 Al-Sadeq International Conference on Multidisciplinary in IT and Communication Science and Applications (AIC-MITCSA). pp. 1–5.

Aljabar, P., Heckemann, R. A., Hammers, A., Hajnal, J. V., Rueckert, D., 2009. Multi-atlas based segmentation of brain images: atlas selection and its effect on accuracy. NeuroImage 46 (3), 726–738.

Altman, D. G., Bland, J. M., 1994. Statistics notes: Diagnostic tests 2: Predictive values. British Medical Journal 309 (6947), 102.

Andermatt, S., Pezold, S., Cattin, P., 2016. Multi-dimensional gated recurrent units for the segmentation of biomedical 3d-data. In: Deep Learning and Data Labeling for Medical Applications. Springer International Publishing, pp. 142–151.

Andermatt, S., Pezold, S., Cattin, P. C., 2018. Automated segmentation of multiple sclerosis lesions using multi-dimensional gated recurrent units. In: Brainlesion: Glioma, Multiple Sclerosis, Stroke and Traumatic Brain Injuries. Springer International Publishing, pp. 31–42.

Ashburner, J., Friston, K. J., 2005. Unified segmentation. NeuroImage 26 (3), 839–851.

Avants, B. B., Tustison, N. J., Song, G., Cook, P. A., Klein, A., Gee, J. C., 2011. A reproducible evaluation of ANTs similarity metric performance in brain image registration. NeuroImage 54 (3), 2033–2044.

Bakshi, R., Thompson, J. A., Rocca, A. M., Pelletier, D., Dousset, V., Barkhof, F., Inglese, M., Guttmann, R. C., Horsfield, A. M., Filippi, M., 2008. MRI in multiple sclerosis: current status and future prospects. The Lancet Neurology 7 (7), 615–625.

Bazin, P.-L., Pham, D. L., 2008. Homeomorphic brain image segmentation with topological and statistical atlases. Medical Image Analysis 12 (5), 616–625.

Beaumont, J., Commowick, O., Barillot, C., 2016a. Automatic multiple sclerosis lesion segmentation from intensity-normalized multi-channel MRI. In: Proceedings of the 1st MICCAI Challenge on Multiple Sclerosis Lesions Segmentation Challenge Using a Data Management and Processing Infrastructure (MICCAI-MSSEG). pp. 9–15.

Beaumont, J., Commowick, O., Barillot, C., 2016b. Multiple sclerosis lesion segmentation using an automated multimodal graph cut. In: Proceedings of the 1st MICCAI Challenge on Multiple Sclerosis Lesions Segmentation Challenge Using a Data Management and Processing Infrastructure (MICCAI-MSSEG). pp. 1–7.

Bezdek, J. C., 1973. Cluster validity with fuzzy sets. Taylor & Francis.

Bland, M., 2015. An introduction to medical statistics. Oxford University Press (UK).

Blystad, I., Håkansson, I., Tisell, A., Ernerudh, J., Smedby, Ö., Lundberg, P., Larsson, E. M., 2016. Quantitative MRI for analysis of active multiple sclerosis lesions without gadolinium-based contrast agent. American Journal of Neuroradiology 37 (1), 94–100.

Boudraa, A.-O., Dehak, S. M. R., Zhu, Y.-M., Pachai, C., Bao, Y.-G., Grimaud, J., 2000. Automated segmentation of multiple sclerosis lesions in multispectral MR imaging using fuzzy clustering. Computers in Biology and Medicine 30 (1), 23–40.

Breiman, L., 2001. Random forests. Machine Learning 45 (1), 5–32.

Brosch, T., Tang, L. Y. W., Yoo, Y., Li, D. K. B., Traboulsee, A., Tam, R., 2016. Deep 3D convolutional encoder networks with shortcuts for multiscale feature integration applied to multiple sclerosis lesion segmentation. IEEE Transactions on Medical Imaging 35 (5), 1229–1239.

Browne, P., Chandraratna, D., Angood, C., Tremlett, H., Baker, C., Taylor, B. V., Thompson, A. J., 2014. Atlas of Multiple Sclerosis 2013: A growing global problem with widespread inequity. Neurology 83 (11), 1022–1024.

Buades, A., Coll, B., Morel, J. M., 2005. A non-local algorithm for image denoising. In: Computer Vision and Pattern Recognition, 2005. CVPR 2005. IEEE Computer Society Conference on. Vol. 2. pp. 60–65.

Buitinck, L., Louppe, G., Blondel, M., Pedregosa, F., Mueller, A., Grisel, O., Niculae, V., Prettenhofer, P., Gramfort, A., Grobler, J., Layton, R., Vanderplas, J., Joly, A., Holt, B., Varoquaux, G., 2013. API design for machine learning software: Experiences from the scikit-learn project. arXiv preprint arXiv:1309.0238.

Calcagno, G., Staiano, A., Fortunato, G., Brescia-Morra, V., Salvatore, E., Liguori, R., Capone, S., Filla, A., Longo, G., Sacchetti, L., 2010. A multilayer perceptron neural network-based approach for the identification of responsiveness to interferon therapy in multiple sclerosis patients. Information Sciences 180 (21), 4153–4163.

Carass, A., Cuzzocreo, J., Wheeler, B. M., Bazin, P.-L., Resnick, S. M., Prince, J. L., 2011. Simple paradigm for extra-cerebral tissue removal: Algorithm and analysis. NeuroImage 56 (4), 1982–1992.

Carass, A., Roy, S., Jog, A., Cuzzocreo, J. L., Magrath, E., Gherman, A., Button, J., Nguyen, J., Prados, F., Sudre, C. H., Cardoso, M. J., Cawley, N., Ciccarelli, O., Wheeler-Kingshott, C. A., Ourselin, S., Catanese, L., Deshpande, H., Maurel, P., Commowick, O., Barillot, C., Tomas-Fernandez, X., Warfield,

S. K., Vaidya, S., Chunduru, A., Muthuganapathy, R., Krishnamurthi, G., Jesson, A., Arbel, T., Maier, O., Handels, H., Iheme, L. O., Unay, D., Jain, S., Sima, D. M., Smeets, D., Ghafoorian, M., Platel, B., Birenbaum, A., Greenspan, H., Bazin, P.-L., Calabresi, P. A., Crainiceanu, C. M., Ellingsen, L. M., Reich, D. S., Prince, J. L., Pham, D. L., 2017. Longitudinal multiple sclerosis lesion segmentation: Resource and challenge. NeuroImage 148, 77–102.

Cárdenes, R., de Luis-García, R., Bach-Cuadra, M., 2009. A multidimensional segmentation evaluation for medical image data. Computer Methods and Programs in Biomedicine 96 (2), 108–124.

Catanese, L., Commowick, O., Barillot, C., 2015. Automatic graph cut segmentation of multiple sclerosis lesions. In: ISBI Longitudinal MS Lesion Segmentation Challenge. pp. 1–2.

Cocosco, C. A., Kollokian, V., Kwan, R. K.-S., Pike, G. B., Evans, A. C., 1997. BrainWeb: Online interface to a 3D MRI simulated brain database. NeuroImage 5, 425.

Collins, D. L., Holmes, C. J., Peters, T. M., Evans, A. C., 1995. Automatic 3D model-based neuroanatomical segmentation. Human Brain Mapping 3 (3), 190–208.

Collins, D. L., Zijdenbos, A. P., Kollokian, V., Sled, J. G., Kabani, N. J., Holmes, C. J., Evans, A. C., 1998. Design and construction of a realistic digital brain phantom. IEEE Transactions on Medical Imaging 17 (3), 463–468.

Commowick, O., Cervenansky, F., Ameli, R., 2016. MSSEG Challenge Proceedings: Multiple Sclerosis Lesions Segmentation Challenge Using a Data Management and Processing Infrastructure. In: International Conference on Medical Image Computing and Computer-Assisted Intervention. pp. 1–95.

Commowick, O., Wiest-Daesslé, N., Prima, S., 2012. Block-matching strategies for rigid registration of multimodal medical images. In: Biomedical Imaging (ISBI), 2012 9th IEEE International Symposium on. pp. 700–703.

Compston, A., Coles, A., 2008. Multiple sclerosis. The Lancet 372 (9648), 1502–1517.

Coupé, P., Yger, P., Prima, S., Hellier, P., Kervrann, C., Barillot, C., 2008. An optimized blockwise nonlocal means denoising filter for 3D magnetic resonance images. IEEE Transactions on Medical Imaging 27 (4), 425–441.

De Boer, R., Vrooman, H. A., Van Der Lijn, F., Vernooij, M. W., Ikram, M. A., Van Der Lugt, A., Breteler, M. M. B., Niessen, W. J., 2009. White matter lesion extension to automatic brain tissue segmentation on MRI. NeuroImage 45 (4), 1151–1161.

Dice, L. R., 1945. Measures of the amount of ecologic association between species. Ecology 26 (3), 297–302.

Ding, L., Goshtasby, A., 2001. On the Canny edge detector. Pattern Recognition 34 (3), 721–725.

Dong, M., Oguz, I., Subbana, N., Calabresi, P., Shinohara, R. T., Yushkevich, P., 2017. Multiple sclerosis lesion segmentation using joint label fusion. In: Patch-Based Techniques in Medical Imaging. Springer International Publishing, pp. 138–145.

Doyle, A., Elliott, C., Karimaghaloo, Z., Subbanna, N., Arnold, D. L., Arbel, T., 2018. Lesion detection, segmentation and prediction in multiple sclerosis clinical trials. In: Brainlesion: Glioma, Multiple Sclerosis, Stroke and Traumatic Brain Injuries. Springer International Publishing, pp. 15–28.

Doyle, S., Forbes, F., Dojat, M., 2016. Automatic multiple sclerosis lesion segmentation with P-LOCUS. In: Proceedings of the 1st MICCAI Challenge on Multiple Sclerosis Lesions Segmentation Challenge Using a Data Management and Processing Infrastructure (MICCAI-MSSEG). pp. 17–20.

Ekin, A., 2006. Feature-based brain mid-sagittal plane detection by RANSAC. In: Signal Processing Conference, 2006 14th European. pp. 1–4.

Eskildsen, S. F., Coup, P., Fonov, V., Manjn, J. V., Leung, K. K., Guizard, N., Wassef, S. N., stergaard, L. R., Collins, D. L., 2012. BEaST: Brain extraction based on nonlocal segmentation technique. NeuroImage 59 (3), 2362 – 2373.

Fazekas, F., Barkhof, F., Filippi, M., Grossman, R. I., Li, D. K. B., McDonald, W. I., McFarland, H. F., Paty, D. W., Simon, J. H., Wolinsky, J. S., Miller, D. H., 1999. The contribution of magnetic resonance imaging to the diagnosis of multiple sclerosis. Neurology 53 (3), 448–456.

Filippi, M., Horsfield, M. A., Tofts, P. S., Barkhof, F., Thompson, A. J., Miller, D. H., 1995. Quantitative assessment of mri lesion load in monitoring the evolution of multiple sclerosis. Brain 118 (6), 1601–1612.

Fischl, B., Salat, D. H., Busa, E., Albert, M., Dieterich, M., Haselgrove, C., Van Der Kouwe, A., Killiany, R., Kennedy, D., Klaveness, S., et al., 2002. Whole brain segmentation: automated labeling of neuroanatomical structures in the human brain. Neuron 33 (3), 341–355.

Fleishman, G. M., Valcarcel, A., Pham, D. L., Roy, S., Calabresi, P. A., Yushkevich, P., Shinohara, R. T., Oguz, I., 2018. Joint intensity fusion image synthesis applied to multiple sclerosis lesion segmentation. In: Brainlesion: Glioma, Multiple Sclerosis, Stroke and Traumatic Brain Injuries. Springer International Publishing, pp. 43–54.

Freire, P. G., Ferrari, R. J., 2016. Automatic iterative segmentation of multiple sclerosis lesions using Student's t mixture models and probabilistic anatomical atlases in FLAIR images. Computers in Biology and Medicine 73, 10–23.

García-Lorenzo, D., Francis, S., Narayanan, S., Arnold, D. L., Collins, D. L., 2013. Review of automatic segmentation methods of multiple sclerosis white matter lesions on conventional magnetic resonance imaging. Medical Image Analysis 17 (1), 1–18.

García-Lorenzo, D., Lecoeur, J., Arnold, D. L., Collins, D. L., Barillot, C., 2009. Multiple sclerosis lesion segmentation using an automatic multimodal graph cuts. In: International Conference on Medical Image Computing and Computer-Assisted Intervention. pp. 584–591.

García-Lorenzo, D., Prima, S., Arnold, L. D., Collins, D. L., Barillot, C., 2011. Trimmed-likelihood estimation for focal lesions and tissue segmentation in multisequence MRI for multiple sclerosis. IEEE Transactions on Medical Imaging 30 (8), 1455–1467.

Ge, Y., 2006. Multiple sclerosis: The role of MR imaging. American Journal of Neuroradiology 27 (6), 1165–1176.

Geremia, E., Menze, B. H., Ayache, N., 2013. Spatially adaptive random forests. In: Biomedical Imaging (ISBI), 2013 IEEE 10th International Symposium on. pp. 1344–1347.

Gerig, G., Jomier, M., Chakos, M., 2001. Valmet: A new validation tool for assessing and improving 3D object segmentation. In: International Conference on Medical Image Computing and Computer-Assisted Intervention. pp. 516–523.

Ghafoorian, M., Platel, B., 2015. Convolutional neural networks for MS lesion segmentation, method description of DIAG team. In: ISBI Longitudinal MS Lesion Segmentation Challenge. pp. 1–2.

Goldberg-Zimring, D., Achiron, A., Miron, S., Faibel, M., Azhari, H., 1998. Automated detection and characterization of multiple sclerosis lesions in brain MR images. Magnetic Resonance Imaging 16 (3), 311–318.

Guizard, N., Coup, P., Fonov, V. S., Manjn, J. V., Arnold, D. L., Collins, D. L., 2015. Rotation-invariant multi-contrast non-local means for MS lesion segmentation. NeuroImage: Clinical 8, 376–389.

Hashemi, R. H., Bradley, W. G., Lisanti, C. J., 2012. MRI: The basics, 3rd Edition. Lippincott Williams & Wilkins.

Havaei, M., Guizard, N., Chapados, N., Bengio, Y., 2016. HeMIS: Hetero-modal image segmentation. In: International Conference on Medical Image Computing and Computer-Assisted Intervention. pp. 469–477.

Hill, J., Matlock, K., Nutter, B., Mitra, S., 2015. Automated segmentation of MS lesions in mr images based on an information theoretic clustering and contrast transformations. Technologies 3 (2), 142–161.

Iheme, L. O., Unay, D., 2015. Automatic white matter hyperintensity segmentation using FLAIR MRI: The MS lesion segmentation challenge. NeuroImage 28 (3), 607–617.

Jenkinson, M., Pechaud, M., Smith, S., 2005. BET2: MR-based estimation of brain, skull and scalp surfaces. In: Eleventh Annual Meeting of the Organization for Human Brain Mapping. Vol. 17. p. 167.

Jesson, A., Arbel, T., 2015. Hierarchical MRF and random forest segmentation of MS lesions and healthy tissues in brain MRI. In: ISBI Longitudinal MS Lesion Segmentation Challenge. pp. 1–3.

Jog, A., Carass, A., Pham, D. L., Prince, J. L., 2015. Multi-output decision trees for lesion segmentation in multiple sclerosis. In: Proceedings of Society of Photographic Instrumentation Engineers (SPIE). pp. 1–10.

Johnson, H., Harris, G., Williams, K., et al., 2007. Insight Journal 57 (1).

Keeli, A. S., Can, A. B., Kaya, A., 2017. A GPU-based approach for automatic segmentation of white matter lesions. IETE Journal of Research, 1–12.

Khademi, A., Venetsanopoulos, A., Moody, A. R., 2012. Robust white matter lesion segmentation in FLAIR MRI. IEEE Transactions on Biomedical Engineering 59 (3), 860–871.

Khademi, A., Venetsanopoulos, A., Moody, A. R., 2014. Generalized method for partial volume estimation and tissue segmentation in cerebral magnetic resonance images. Journal of Medical Imaging 1 (1), 1–17.

Khotanlou, H., Colliot, O., Atif, J., Bloch, I., 2009. 3D brain tumor segmentation in MRI using fuzzy classification, symmetry analysis and spatially constrained deformable models. Fuzzy Sets and Systems 160 (10), 1457–1473.

Knight, J., Khademi, A., 2016. Ms lesion segmentation using FLAIR MRI only. In: Proceedings of the 1st MICCAI Challenge on Multiple Sclerosis Lesions Segmentation Challenge Using a Data Management and Processing Infrastructure (MICCAI-MSSEG). pp. 21–28.

Koch, G. G., 1982. Encyclopedia of Statistical Sciences. John Wiley and Sons.

Koley, S., Chakraborty, C., Mainero, C., Fischl, B., Aganj, I., 2016. A fast approach to automatic detection of brain lesions. In: International Conference on Medical Image Computing and Computer-Assisted Intervention Brain Lesions Workshop. pp. 1–9.

Kwan, R. K. S., Evans, A. C., Pike, G. B., 1996. An extensible MRI simulator for post-processing evaluation. In: Visualization in Biomedical Computing. pp. 135–140.

Kwan, R. K. S., Evans, A. C., Pike, G. B., 1999. MRI simulation-based evaluation of image-processing and classification methods. IEEE Transactions on Medical Imaging 18 (11), 1085–1097.

Lao, Z., Shen, D., Liu, D., Jawad, A. F., Melhem, E. R., Launer, L. J., Bryan, R. N., Davatzikos, C., 2008. Computer-assisted segmentation of white matter lesions in 3D MR images using support vector machine. Academic Radiology 15 (3), 300–313.

Li, C., Gatenby, C., Wang, L., Gore, J. C., 2009. A robust parametric method for bias field estimation and segmentation of mr images. In: 2009 IEEE Conference on Computer Vision and Pattern Recognition. pp. 218–223.

Lladó, X., Ganiler, O., Oliver, A., Martí, R., Freixenet, J., Valls, L., Vilanova, J. C., Ramió-Torrentà, L., Rovira, À., 2012a. Automated detection of multiple sclerosis lesions in serial brain MRI. Neuroradiology 54 (8), 787–807.

Lladó, X., Oliver, A., Cabezas, M., Freixenet, J., Vilanova, J. C., Quiles, A., Valls, L., Ramió-Torrentí, L., Rovira, À., 2012b. Segmentation of multiple sclerosis lesions in brain MRI: A review of automated approaches. Information Sciences 186 (1), 164–185.

Ma, K. C., Fernandez, J. R., Amezcua, L., Lerner, A., Shiroishi, M. S., Liu, B. J., 2015. Design and development of an ethnically-diverse imaging informatics-based efolder system for multiple sclerosis patients. Computerized Medical Imaging and Graphics 46, 257 – 268.

Mahbod, A., Wang, C., Örjan Smedby, 2016. Automatic multiple sclerosis lesion segmentation using hybrid artificial neural networks. In: Proceedings of the 1st MICCAI Challenge on Multiple Sclerosis Lesions Segmentation Challenge Using a Data Management and Processing Infrastructure (MICCAI-MSSEG). pp. 29–36.

Maier, O., Handels, H., 2015. MS lesion segmentation in MRI with random forests. In: ISBI Longitudinal MS Lesion Segmentation Challenge. pp. 1–2.

Manjón, J. V., Coupé, P., 2016. volBrain: An online MRI brain volumetry system. Frontiers in Neuroinformatics 10 (30), 1–14.

Marr, D., Hildreth, E., 1980. Theory of edge detection. Proceedings of the Royal Society of London B: Biological Sciences 207 (1167), 187–217.

Martola, J., Bergström, J., Fredrikson, S., Stawiarz, L., Hillert, J., Zhang, Y., Flodmark, O., Lilja, A., Ekbom, A., Aspelin, P., Wiberg, M. K., 2010. A longitudinal observational study of brain atrophy rate reflecting four decades of multiple sclerosis: a comparison of serial 1D, 2D, and volumetric measurements from MRI images. Neuroradiology 52 (2), 109–117.

Mazziotta, J., Toga, A., Evans, A., Fox, P., Lancaster, J., Zilles, K., Woods, R., Paus, T., Simpson, G., Pike, B., Holmes, C., Collins, L., Thompson, P., MacDonald, D., Iacoboni, M., Schormann, T., Amunts, K., Palomero-Gallagher, N., Geyer, S., Parsons, L., Narr, K., Kabani, N., Goualher, G. L.,

Boomsma, D., Cannon, T., Kawashima, R., Mazoyer, B., 2001. A probabilistic atlas and reference system for the human brain: International Consortium for Brain Mapping (ICBM). Philosophical Transactions of the Royal Society of London B: Biological Sciences 356 (1412), 1293–1322.

McKinley, R., Gundersen, T., Wagner, F., Chan, A., Wiest, R., Reyes, M., 2016. Nabla-net: A deep dag-like convolutional architecture for biomedical image segmentation: Application to white-matter lesion segmentation in multiple sclerosis. In: Proceedings of the 1st MICCAI Challenge on Multiple Sclerosis Lesions Segmentation Challenge Using a Data Management and Processing Infrastructure (MICCAI-MSSEG). pp. 37–43.

Meier, D. S., Guttmann, C. R., Tummala, S., Moscufo, N., Cavallari, M., Tauhid, S., Bakshi, R., Weiner, H. L., 2017. Dual-Sensitivity Multiple Sclerosis Lesion and CSF Segmentation for Multichannel 3T Brain MRI. Journal of Neuroimaging 28 (1), 36–47.

Mortazavi, D., Kouzani, A. Z., Soltanian-Zadeh, H., 2012. Segmentation of multiple sclerosis lesions in MR images: A review. Neuroradiology 54 (4), 299–320.

Muschelli, J., Sweeney, E., Maronge, J., Crainiceanu, C., 2016. Prediction of MS lesions using random forests. In: Proceedings of the 1st MICCAI Challenge on Multiple Sclerosis Lesions Segmentation Challenge Using a Data Management and Processing Infrastructure (MICCAI-MSSEG). pp. 45–50.

Noseworthy, J. H., Lucchinetti, C., Rodriguez, M., Weinshenker, B. G., 2000. Multiple sclerosis. New England Journal of Medicine 343 (13), 938–952.

Notsu, A., Komori, O., Eguchi, S., 2014. Spontaneous clustering via minimum gamma-divergence. Neural Computation 26 (2), 421–448.

Perona, P., Malik, J., 1990. Scale-space and edge detection using anisotropic diffusion. IEEE Transactions on Pattern Analysis and Machine Intelligence 12 (7), 629–639.

Polman, C. H., Reingold, S. C., Banwell, B., Clanet, M., Cohen, J. A., Filippi, M., Fujihara, K., Havrdova, E., Hutchinson, M., Kappos, L., Lublin, F. D., Montalban, X., OConnor, P., Sandberg-Wollheim, M., Thompson, A. J., Waubant, E., Weinshenker, B., Wolinsky, J. S., 2011. Diagnostic criteria for multiple sclerosis: 2010 revisions to the McDonald criteria. Annals of Neurology 69 (2), 292–302.

Prados, F., Cardoso, M., Cawley, N., Ciccarelli, O., Wheeler-Kingshott, C., Ourselin, S., 2015. Multi-contrast patchmatch algorithm for multiple sclerosis lesion detection. In: ISBI Longitudinal MS Lesion Segmentation Challenge. pp. 1–2.

Rodrigo, F., Filipuzzi, M., Isoardi, R., Noceti, M., Graffigna, J. P., 2013. High intensity region segmentation in MR imaging of multiple sclerosis. Journal of Physics: Conference Series 477 (1), 1–8.

Roura, E., Cabezas, M., Valverde, S., González-Villá, S., Salvi, J., Oliver, A., Lladó, X., 2016. Unsupervised multiple sclerosis lesion detection and segmentation using rules and level sets. In: Proceedings of the 1st MICCAI Challenge on Multiple Sclerosis Lesions Segmentation Challenge Using a Data Management and Processing Infrastructure (MICCAI-MSSEG). pp. 51–56.

Roura, E., Oliver, A., Cabezas, M., Valverde, S., Pareto, D., Vilanova, J. C., Ramió-Torrentà, L., Rovira, À., Lladó, X., 2015. A toolbox for multiple sclerosis lesion segmentation. Neuroradiology 57 (10), 1031–1043.

Rovira, À., León, A., 2008. MR in the diagnosis and monitoring of multiple sclerosis: An overview. European Journal of Radiology 67 (3), 409–414.

Rovira, À., Swanton, J., Tintoré, M., Huerga, E., Barkhof, F., Filippi, M., Frederiksen, J. L., Langkilde, A., Miszkiel, K., Polman, C., Rovaris, M., Sastre-Garriga, J., Miller, D., Montalban, X., 2009. A single, early magnetic resonance imaging study in the diagnosis of multiple sclerosis. Archives of Neurology 66 (5), 587–592.

Roy, S., Bandyopadhyay, S. K., Bhattacharyya, D., Kim, T. H., 2016. An improved brain MR image binarization method as a preprocessing for abnormality detection and features extraction. Frontiers of Computer Science, 1–12.

Roy, S., Bhattacharyya, D., Bandyopadhyay, S. K., Kim, T.-H., 2017a. An effective method for computerized prediction and segmentation of multiple sclerosis lesions in brain MRI. Computer Methods and Programs in Biomedicine 140, 307–320.

Roy, S., Butman, J. A., Pham, D. L., 2017b. Robust skull stripping using multiple mr image contrasts insensitive to pathology. NeuroImage 146, 132–147.

Roy, S., Butman, J. A., Reich, D. S., Calabresi, P. A., Pham, D. L., 2018. Multiple Sclerosis Lesion Segmentation from Brain MRI via Fully Convolutional Neural Networks. arXiv:1803.09172 [cs.CV].

Roy, S., Nag, S., Bandyopadhyay, S. K., Bhattacharyya, D., Kim, T.-H., 2015. Automated brain hemorrhage lesion segmentation and classification from mr image using an innovative composite method. Journal of Theoretical and Applied Information Technology 78 (1), 34–45.

Roy, S., Nag, S., Maitra, I. K., Bandyopadhyay, S. K., 2013. Artefact removal and skull elimination from MRI of brain image. International Journal of Scientific and Engineering 4, 163–170.

Sahraian, M. A., Radue, E.-W., 2008. MRI atlas of MS lesions. Springer.

Salembier, P., Oliveras, A., Garrido, L., 1998. Antiextensive connected operators for image and sequence processing. IEEE Transactions on Image Processing 7 (4), 555–570.

Santos, M. M., Diniz, P. R. B., Silva-Filho, A. G., Santos, W. P., 2016. Evaluation-oriented training strategy on MS segmentation challenge 2016. In: Proceedings of the 1st MICCAI Challenge on Multiple Sclerosis Lesions Segmentation Challenge Using a Data Management and Processing Infrastructure (MICCAI-MSSEG). pp. 57–62.

Schmidt, P., Gaser, C., Arsic, M., Buck, D., Frschler, A., Berthele, A., Hoshi, M., Ilg, R., Schmid, V. J., Zimmer, C., Hemmer, B., Mhlau, M., 2012. An automated tool for detection of FLAIR-hyperintense white-matter lesions in multiple sclerosis. NeuroImage 59 (4), 3774–3783.

Shiee, N., Bazin, P.-L., Ozturk, A., Reich, D. S., Calabresi, P. A., Pham, D. L., 2010. A topology-preserving approach to the segmentation of brain images with multiple sclerosis lesions. NeuroImage 49 (2), 1524–1535.

Simon, J. H., Li, D., Traboulsee, A., Coyle, P. K., Arnold, D. L., Barkhof, F., Frank, J. A., Grossman, R., Paty, D. W., Radue, E. W., Wolinsky, J. S., 2006. Standardized MR imaging protocol for multiple sclerosis: Consortium of MS centers consensus guidelines. American Journal of Neuroradiology 27 (2), 455–461.

Sled, J. G., Zijdenbos, A. P., Evans, A. C., 1998. A nonparametric method for automatic correction of intensity nonuniformity in MRI data. IEEE Transactions on Medical Imaging 17 (1), 87–97.

Smith, S. M., 2002. Fast robust automated brain extraction. Human brain mapping 17 (3), 143–155.

Steenwijk, M. D., Pouwels, P. J., Daams, M., van Dalen, J. W., Caan, M. W., Richard, E., Barkhof, F., Vrenken, H., 2013. Accurate white matter lesion segmentation by k nearest neighbor classification with tissue type priors (kNN-TTPs). NeuroImage: Clinical 3, 462–469.

Stokking, R., Vincken, K. L., Viergever, M. A., 2000. Automatic morphology-based brain segmentation (MBRASE) from MRI-T1 data. NeuroImage 12 (6), 726–738.

Storelli, L., Pagani, E., Rocca, M., Horsfield, M. A., Gallo, A., Bisecco, A., Battaglini, M., Stefano, N. D., Vrenken, H., Thomas, D. L., Mancini, L., Ropele, S., Enzinger, C., Preziosa, P., Filippi, M., 2016. A semiautomatic method for multiple sclerosis lesion segmentation on dual-echo MR imaging:

Application in a multicenter context. American Journal of Neuroradiology 38 (2), 1–7.

Strumia, M., Schmidt, F. R., Anastasopoulos, C., Granziera, C., Krueger, G., Brox, T., 2016. White matter MS-lesion segmentation using a geometric brain model. IEEE Transactions on Medical Imaging 35 (7), 1636–1646.

Styner, M., Lee, J., Chin, B., Chin, M., Commowick, O., Tran, H., Markovic-Plese, S., Jewells, V., Warfield, S., 2008. 3D segmentation in the clinic: A grand challenge ii: MS lesion segmentation. MIDAS, 1–6.

Subbanna, N., Precup, D., Arnold, D., Arbel, T., 2015. IMaGe: Iterative multi-level probabilistic graphical model for detection and segmentation of multiple sclerosis lesions in brain MRI. In: International Conference on Information Processing in Medical Imaging. pp. 514–526.

Sugar, C. A., James, G. M., 2003. Finding the number of clusters in a dataset: An information-theoretic approach. Journal of the American Statistical Association 98 (463), 750–763.

Summers, D., 2003. Whole Brain Atlas: www.med.harvard.edu/AANLIB/home.html. Journal of Neurology, Neurosurgery, and Psychiatry 74 (3), 288.

Ta, V.-T., Giraud, R., Collins, D. L., Coupé, P., 2014. Optimized PatchMatch for near real time and accurate label fusion. In: International Conference on Medical Image Computing and Computer-Assisted Intervention. pp. 105–112.

Tadayon, E., (Khayati), R. M., Karami, V., Nabavi, S. M., 2016. A novel method for automatic classification of multiple sclerosis lesion subtypes using diffusion tensor MR images. Biomedical Engineering: Applications, Basis and Communications 28 (5), 1–13.

Taha, A. A., Hanbury, A., 2015. Metrics for evaluating 3D medical image segmentation: analysis, selection, and tool. BMC Medical Imaging 15 (1), 29–55.

Tian, W., Zhu, T., Zhong, J., Liu, X., Rao, P., Segal, B. M., Ekholm, S., 2012. Progressive decline in fractional anisotropy on serial DTI examinations of the corpus callosum: a putative marker of disease activity and progression in SPMS. Neuroradiology 54 (4), 287–297.

Tomas-Fernandez, X., Warfield, S. K., 2015. A model of population and subject (MOPS) intensities with application to multiple sclerosis lesion segmentation. IEEE Transactions on Medical Imaging 34 (6), 1349–1361.

Tomas-Fernandez, X., Warfield, S. K., 2016. MRI robust brain tissue segmentation with application to multiple sclerosis. In: Proceedings of the 1st MICCAI Challenge on Multiple Sclerosis Lesions Segmentation Challenge Using a Data Management and Processing Infrastructure (MICCAI-MSSEG). pp. 63–67.

Tustison, N. J., Avants, B. B., Cook, P. A., Zheng, Y., Egan, A., Yushkevich, P. A., Gee, J. C., 2010. N4ITK: improved N3 bias correction. IEEE Transactions on Medical Imaging 29 (6), 1310–1320.

Udupa, J. K., Leblanc, V. R., Zhuge, Y., Imielinska, C., Schmidt, H., Currie, L. M., Hirsch, B. E., Woodburn, J., 2006. A framework for evaluating image segmentation algorithms. Computerized Medical Imaging and Graphics 30 (2), 75–87.

Urien, H., Buvat, I., Rougon, N., Bloch, I., 2016. A 3D hierarchical multimodal detection and segmentation method for multiple sclerosis lesions in MRI. In: Proceedings of the 1st MICCAI Challenge on Multiple Sclerosis Lesions Segmentation Challenge Using a Data Management and Processing Infrastructure (MICCAI-MSSEG). pp. 69–73.

Valverde, S., Cabezas, M., González-Villá, S., Salvi, J., Oliver, A., Lladó, X., 2016. Multiple sclerosis lesion detection and segmentation using a convolutional neural network of 3D patches. In: Proceedings of the 1st MICCAI Challenge on Multiple Sclerosis Lesions Segmentation Challenge Using a Data Management and Processing Infrastructure (MICCAI-MSSEG). pp. 75–79.

Valverde, S., Cabezas, M., Roura, E., González-Villá, S., Pareto, D., Vilanova, J. C., Ramió-Torrentá, L., Álex Rovira, Oliver, A., Lladó, X., 2017. Improving automated multiple sclerosis lesion segmentation with a cascaded 3D convolutional neural network approach. NeuroImage 155, 159–168.

Van Den Elskamp, I. J., Boden, B., Dattola, V., Knol, D. L., Filippi, M., Kappos, L., Fazekas, F., Wagner, K., Pohl, C., Sandbrink, R., Polman, C. H., Uitdehaag, B. M. J., Barkhof, F., 2010. Cerebral atrophy as outcome measure in short-term phase 2 clinical trials in multiple sclerosis. Neuroradiology 52 (10), 875–881.

Van Leemput, K., Maes, F., Vandermeulen, D., Colchester, A., Suetens, P., 2001. Automated segmentation of multiple sclerosis lesions by model outlier detection. IEEE transactions on medical imaging 20 (8), 677–688.

Vera-Olmos, F. J., Melero, H., N.Malpica, 2016. Random forest for multiple sclerosis lesion segmentation. In: Proceedings of the 1st MICCAI Challenge on Multiple Sclerosis Lesions Segmentation Challenge Using a Data Management and Processing Infrastructure (MICCAI-MSSEG). pp. 81–86.

Vrenken, H., Jenkinson, M., Horsfield, M. A., Battaglini, M., Van Schijndel, R. A., Rostrup, E., Geurts, J. J. G., Fisher, E., Zijdenbos, A., Ashburner, J., Miller, D. H., Filippi, M., Fazekas, F., Rovaris, M., Rovira, À., Barkhof, F., De Stefano, N., MAGNIMS Study Group, 2013. Recommendations to improve imaging and analysis of brain lesion load and atrophy in longitudinal studies of multiple sclerosis. Journal of Neurology 260 (10), 2458–2471.

Wack, D. S., Dwyer, M. G., Bergsland, N., Di Perri, C., Ranza, L., Hussein, S., Ramasamy, D., Poloni, G., Zivadinov, R., 2012. Improved assessment of multiple sclerosis lesion segmentation agreement via detection and outline error estimates. BMC Medical Imaging 12 (1), 17.

Wang, H., Suh, J. W., Das, S. R., Pluta, J. B., Craige, C., Yushkevich, P. A., 2013. Multi-atlas segmentation with joint label fusion. IEEE Transactions on Pattern Analysis and Machine Intelligence 35 (3), 611–623.

Weiss, N., Rueckert, D., Rao, A., 2013. Multiple Sclerosis Lesion Segmentation Using Dictionary Learning and Sparse Coding. Springer Berlin Heidelberg, pp. 735–742.

World Health Organization (WHO) and Multiple Sclerosis International Federation, 2008. Atlas. Multiple sclerosis resources in the world, 2008. World Health Organization.

Wu, Y., Warfield, S. K., Tan, I. L., Wells III, W. M., Meier, D. S., van Schijndel, R. A., Barkhof, F., Guttmann, C. R., 2006. Automated segmentation of multiple sclerosis lesion subtypes with multichannel MRI. NeuroImage 32 (3), 1205–1215.

Yoo, T. S., Ackerman, M. J., Lorensen, W. E., Schroeder, W., Chalana, V., Aylward, S., Metaxas, D., Whitaker, R., 2002. Engineering and algorithm design for an image processing API: A technical report on ITK-the insight toolkit. Studies in Health Technology and Informatics, 586–592.

Younis, A., Ibrahim, M., Kabuka, M., John, N., 2008. An artificial immune-activated neural network applied to brain 3D MRI segmentation. Journal of Digital Imaging 21 (1), 69–88.

Yu, X., Yla-Jaaski, J., 1991. A new algorithm for image segmentation based on region growing and edge detection. In: Circuits and Systems, 1991, IEEE International Symposium on. pp. 516–519.

Zivadinov, R., Stosic, M., Cox, J. L., Ramasamy, D. P., Dwyer, M. G., 2008. The place of conventional MRI and newly emerging mri techniques in monitoring different aspects of treatment outcome. Journal of Neurology 255 (1), 61–74.